ITR-1529

PRELIMINARY REPORT

OPERATION PLUMBBOB

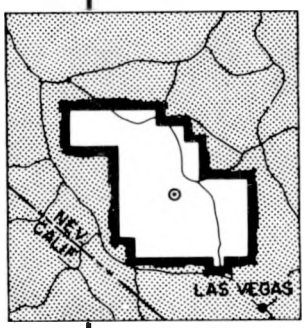

NEVADA TEST SITE
MAY–OCTOBER 1957

Project 26.4b

SUBSURFACE MOTION FROM A CONFINED UNDERGROUND DETONATION—PART I

Issuance Date: November 25, 1958

SANDIA CORPORATION · ALBUQUERQUE, NEW MEXICO

This is a preliminary report based on all data available at the close of this project's participation in Operation PLUMBBOB. The contents of this report are subject to change upon completion of evaluation for the final report. This preliminary report will be superseded by the publication of the final (WT) report. Conclusions and recommendations drawn herein, if any, are therefore tentative. The work is reported at this early time to provide early test results to those concerned with the effects of nuclear weapons and to provide for an interchange of information between projects for the preparation of final reports.

AEC Technical Information Service Extension
Oak Ridge, Tennessee

Operation PLUMBBOB Interim Report

Project 26.4b

SUBSURFACE MOTION FROM A CONFINED UNDERGROUND DETONATION — PART I

By

William R. Perret

Approved by: M. L. MERRITT, Weapons Effects Department

Sandia Corporation
Albuquerque, New Mexico
October 1957

ABSTRACT

Strong motion observations within the mesa adjacent to Rainier shot of Operation Plumbbob (1.7 kt) were made on a horizontal radius (along the access tunnel) and a vertical radius by Sandia Corporation under Project 26.4b. Principal data were derived from radial component acceleration measurements. Long-base strain gages provided some secondary data. Horizontal radius data were derived from gages at distances ranging from 100 to 1,355 feet from the burst point. Vertical radius data were obtained over distances ranging from 366 to 896 feet at the mesa top surface.

Many of the accelerometers used in Project 26.4b were given set ranges so far below actual peak accelerations that recorder system overloading caused saturation and serious loss of precision in record peak amplitudes. All arrival time data are good, but amplitude data are questionable in many cases. Accelerometers at closer stations on both radii were not seriously overranged and data from them are reliable. Corrections based on a few records from Project 26.4a (SRI) gages of a vertical radius installation were made for the overranged Project 26.4b gages of the vertical radius. Corrected and uncorrected acceleration-time data for the vertical radius gages were converted to particle velocity and displacement information by integration.

Horizontal radius data show peak accelerations decreasing approximately as the inverse fourth power of radial range between about 3,500 g at 100 feet and 10 g at, roughly, 400 feet where the rate of decrease approaches the inverse square of range.

Peak accelerations from the vertical radius decrease with range up to the vicinity of transition from weak bedded tuff to the welded tuff (rhyolite) cap rock. From this region upward toward the surface record, character changes radically. A sharp upward acceleration pulse is followed by a relatively long period of free fall at about -1 g (true zero g for the accelerometer biased to +1 g in calibration). A sharp upward rebound pulse and a decaying oscillatory train complete the motion. Free fall originates at all gages nearly simultaneously but ends at progressively later times upward.

Rebound initiation sequence suggests that horizontal parting or spalling occurred at three levels from beneath the cap rock upward to the surface.

Initial peak accelerations through the cap rock region increase with increasing radial range. This cannot be attributed to surface reflection except at the surface gage. The anomalous increase in amplitude may be caused by continuously decreasing seismic impedance (ρc) upward through the cap rock, with consequent continuous reflection of the compression wave with enhanced peaks.

Horizontal strain gages on the tunnel walls survived for periods too short to observe significant motion. Strain gages on the vertical radius showed significant, but small, compressive strains; however, they may have been constrained from free tensile motions by mounting cables.

PREFACE

Project 26.4b was a part of the strong motion studies program under Dr. Roger G. Preston, Director of Program 26, sponsored by the Radiation Laboratory of the University of California, Livermore (UCRL), in conjunction with their Rainier experiment during Operation Plumbbob.

This project was planned by Sandia Corporation in cooperation with UCRL and other agencies participating in the strong motion program. It was executed by the Field Test Organization of Sandia Corporation. Joe W. Wistor served as project officer. Other members of the field party included Harry E. Bell, Ross R. French, W. Keith McCoy, John H. Morrison, and Clarence R. Pickens. Data reduction was performed under supervision of Robert J. Beyatte. The author served as scientific officer of the project and as one of the scientific advisors for the Rainier event.

CONTENTS

CONTENTS (Continued)

ILLUSTRATIONS

ILLUSTRATIONS (Continued)

CHAPTER 6 RESULTS

TABLES

CHAPTER 4 INSTALLATION OF INSTRUMENTS

CHAPTER 5 DATA

CHAPTER 6 RESULTS

Chapter 1

OBJECTIVE AND BACKGROUND

Rainier event of operation Plumbbob was a nuclear explosion deep within a massive layer of tuff (rock formed of volcanic ash)[1]. The primary purpose of this shot was to study the effectiveness of such an environment for containment of radioactive products of nuclear explosions, with consequent elimination of fallout contamination problems from diagnostic testing. This program approached a completely unexplored region of underground explosion phenomena and consequently the initial test was restricted to a device of relatively small energy yield. Extension of the technique to testing devices of larger yields would be based, to a considerable extent, on success of the Rainier event. Scaling from measurements of various shock-induced parameters in the rock would facilitate extension of the technique.

The Rainier device was located in a small room at the end of a tunnel driven horizontally into a large flat-topped mesa in Area 12 (Figure 1.1) near the northwestern corner of Nevada Test Site (NTS). The explosion was 900 feet below the mesa top and about 1,675 feet from the tunnel portal. The shortest distance to the sloping face of the mesa from the explosion was about 900 feet at a point near the interface between the hard welded-tuff (rhyolite) cap rock and the softer tuff which composed most of the mesa (Figure 1.2).

1.1 PURPOSE AND SCOPE OF PROJECT 26.4b

Project 26.4b was one of several projects[2] designed to provide data concerning the strong motion within the rock and over the ground surface in the vicinity of Rainier shot. These data would provide a basis for estimating feasibility of future tests and for design criteria. They would also furnish empirical foundations for more effective scientific studies of response of rocks to the explosive release of extremely high energies. Specifically, this project was concerned with observation of radial motion along a horizontal and a vertical radius.

1.2 BACKGROUND

Underground explosions have customarily served any of three purposes: (a) development of craters and excavation, (b) demolition of structures and other facilities, and (c) generation of seismic pulses for exploration of subsurface geology. Each of these fields has developed a literature confined, with few exceptions, to chemical explosives and, with the exception of exploration seismology, dealing almost solely with empirical results of experimental or applied usage.

Exploration seismology is concerned, logically, with the more remote reactions of relatively shallow crustal layers of the earth to explosions. Its literature includes a strong theoretical component dealing with the generation and transmission of seismic pulses from confined

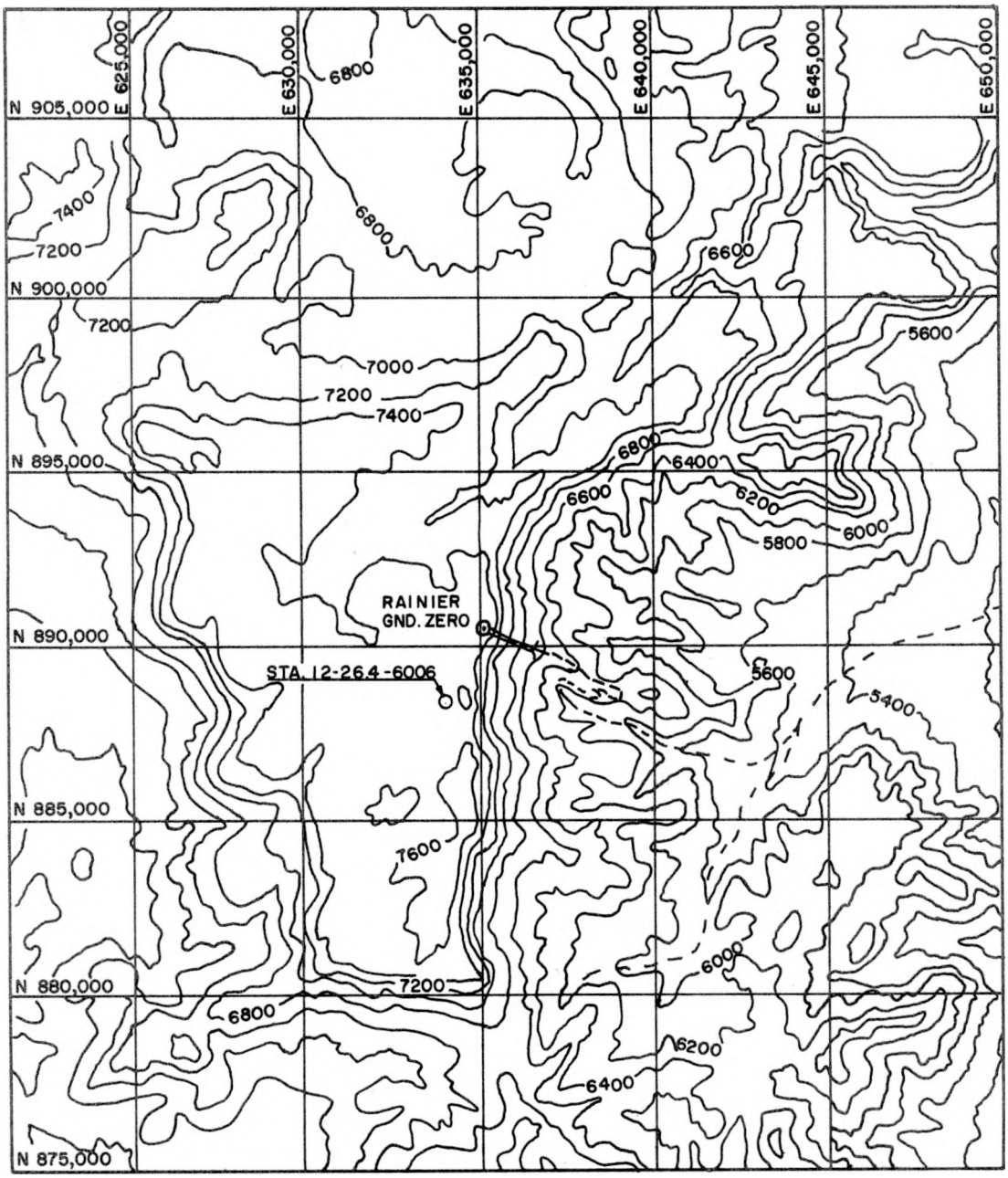

Fig. 1.1—Site map, Area 12.

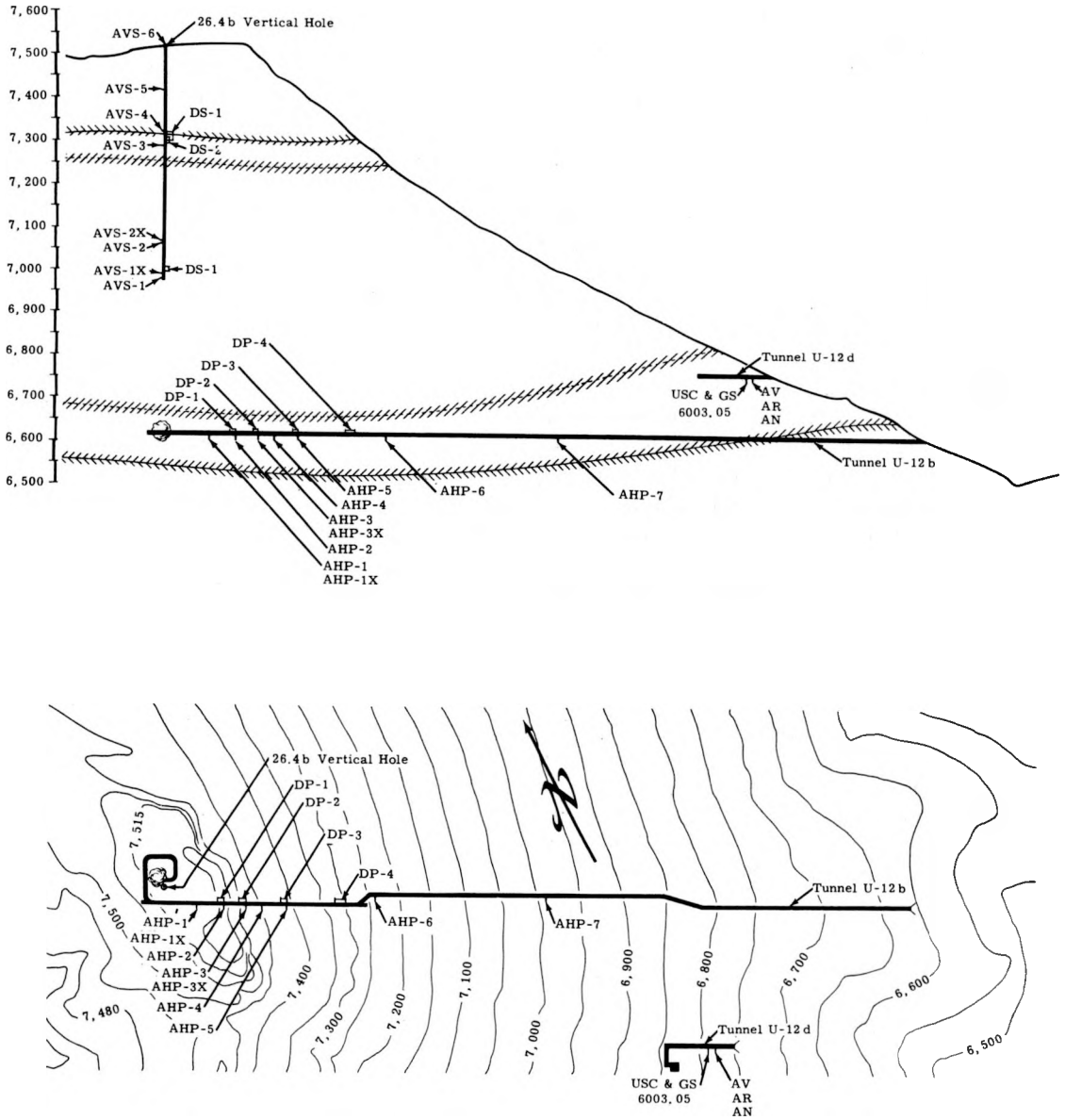

Fig. 1.2—Plan and elevation, Rainier tunnel.

explosions. Several noteworthy studies of interaction of explosions with immediately surrounding rock have resulted from the specific needs of exploration seismology.[3]

Experimental work with high explosives accomplished by Department of Defense agencies has produced data concerning motion of the ground surrounding an explosion at distances of the order of two to ten radial scale factors; i.e., $R/W^{1/3}$ measured in $ft/lb^{1/3}$, where R is radial distance and W is energy yield in equivalent weight of TNT. The sandstone phase of the Underground Explosion Test program (UET) completed by the Corps of Engineers, U.S. Army, in 1952,[4] is particularly pertinent in its correlation of peak acceleration with radial distance and material density for explosions up to 160 tons of TNT.

A major factor in comparison of chemical with nuclear explosions is the enormously greater energy density achieved by the latter and the consequent requirement that the equation of state of the medium within which the explosion occurs must be extended through much higher ranges of temperature and pressure. This situation probably affects directly the phenomena close to the explosive, perhaps within a scaled radius, but it may also affect more remote reactions of the medium through differences in duration. Several theoretical prediction studies of the very close effects of a nuclear explosion underground were made prior to Operation Jangle.[5]

Experimental observations of acceleration and soil stresses were made for two shallow underground nuclear explosions[6, 7] and in several programs of underground high explosives tests, notably Project Mole,[8] a sequel of the UET program. These data were, in general, not applicable to prediction of effects from a deep underground explosion such as Rainier because each was in soil rather than in rock, and each vented to form a crater and produced appreciable air blast with consequent externally induced ground motion.

Two test shots of 10 and 50 tons of 60-percent dynamite gelatin were detonated by the U.S. Geological Survey (USGS) in tunnels in Oak Spring tuff prior to Rainier to furnish rough empirical data concerning gross effects and a few measurements of acceleration.[9, 10] These HE shots did not permit direct correlation with the proposed nuclear shot because they were relatively much shallower, and existing zones of weakness in the rock at the HE test site were relatively much more significant to ground motion than the less numerous faults at the nuclear site. However, results of the preliminary shots, and particularly of those for the larger one (50 tons), fixed an upper limit of gross surface motion and fracturing with reasonable containment. Studies of the gross motion and observed accelerations from the 50-ton shot,[10] considered in the light of the uncertainties of scaling between HE and nuclear bursts, suggested upper limits of vertical motion at ground zero (above the burst) of about 4 feet and peak vertical accelerations at the surface of the order of 10 to 15 g's.

Chapter 2

PLAN OF THE EXPERIMENT

2.1 GENERAL PLAN OF STRONG MOTION OBSERVATIONS

It was evident early in the planning for Rainier that an effective program to provide information for later, larger yield, diagnostic underground shots must include data from (a) the immediate vicinity of the burst where vaporization, melting, and strong plastic deformation were expected; (b) an intermediate region beyond the zone of major physical alteration and extending to the ground surface; and (c) a more remote region extending from surface zeros on the mesa top and slope to distances as great as 100 miles. The first region, involving extremely violent reactions corresponding, at least in part, to fireball problems, was assigned to Program 25, Armour Research Foundation (ARF). The second region and part of the third, involving transition from extremely high accelerations and large plastic deformations to predominantly elastic motion, were the domain of Program 26.

Program 26 included all the strong motion studies and much collateral work. The 26.4 projects comprised strong motion studies, of which: Project 26.4a, Stanford Research Institute (SRI), observed surface motions and strains from ground zero to a ground range of about 2,500 feet, and included observation of motion on a vertical radius to a depth of about 400 feet; Project 26.4b, Sandia Corporation (SC), observed ground motion and strains on a vertical radius which extended from the surface to a point about 370 feet above the device and over a range from 100 feet to the surface on a horizontal radius; Project 26.4d,* U.S. Coast and Geodetic Survey (USC &GS), measured three components of ground motion at stations, generally on the surface, over ground ranges from about 1,250 feet to 17,000 feet; Project 26.4e, Engineer Research and Development Laboratory (ERDL), included measurements of ground motion, strains, and pressures on a horizontal radius, beginning 75 feet from zero and paralleling Project 26.4b but not, in general, duplicating the latter; and, finally, Project 26.4f, Edgerton, Germeshausen and Grier, Incorporated (EG&G), observed gross movement of the surface photographically.

These projects were all tied together at one or more duplicate stations to assure continuity of data and, as in the case of observations on the vertical radius included in 26.4a, to furnish positive back-up in regions where there was a priori reason to anticipate some loss of data.

*Project 26.4c was deleted in the initial planning of the strong motion measurement program.

2.2 DESCRIPTION OF PROJECT 26.4b

Primary measurements of Project 26.4b were radial accelerations on a vertical and a horizontal radius extending, as planned, from points about 100 feet from the device approximately to the ground surface. At one station, in the recording tunnel, U-12-d, near the main tunnel and about 1,350 feet from the device, three components of acceleration (radial, vertical, and tangential) were observed adjacent to Project 26.4d Station 05. Long-base (10- or 20-foot) strain measurements were made at four stations on the horizontal radius and at three stations on the vertical one (Fig. 1.2).

In addition to direct measurements of motion, three collateral observations were undertaken. Zero-time determination by means of a blast switch signal derived from within the device room was undertaken as a refinement to the EG&G zero-time relay signal. Time-of-break measurements were planned to fix the time at which the tunnel wall adjacent to the device room collapsed. These measurements were abandoned because the available recording system was not compatible with the anticipated requirement for time resolution, and development of a suitable facility could not have been effectively accomplished within the prescribed time. Several recording channels were made available to Project 26.3, Broadview Research and Development (BRD), for experimental observation of shock-generated transient temperatures within 600 feet of the explosion.

2.2.1 Gage Identification

Each instrument, with its assigned information channel of Project 26.4b, was identified by a code which indicated type, direction, and order of instrument position in each of the two radial arrays. Accelerometers were designated by A; relative displacement gages, also classified as long-base strain gages, by D. Codes for gages responding to vertical motion included V; horizontal motion, H. Gages were numbered in sequence with increasing range, starting with 1 nearest the burst point in each array. Codes for all gages in the horizontal tunnel group included P; for the vertical boring group, S. Thus, the deepest gage of those in the vertical boring was an accelerometer designated by AVS-1; the corresponding gage in the tunnel was AHP-1. Displacement gages were numbered independently; thus, DP-1 was adjacent to AHP-2. Displacement gages did not carry a symbol to differentiate direction; however, all DS gages responded to vertical motion, and DP gages to horizontal motion.

Accelerometers at the U-12-d tunnel station are identified only as AV, AR, and AN, responding respectively to vertical, radial, and tangential components of motion.

Positions of the gages are indicated in Fig. 1.2. Ranges and depths are listed in the data tables of Chapter 5.

2.3 SET RANGE DETERMINATION

Set range estimates for acceleration measurements in rock for Program 26 were based principally on two sets of experimental data. One of these, UET data from the Castledale Sandstone Test,[4] was used principally for the close-in instrumentation. The other data, derived from high-explosive pilot tests for Rainier by the USGS,[9,10] established ranges for more remote observations. UET data were used independently for Projects 26.4a, 26.4b, and 26.4e with somewhat different, though comparable, results. Differences consisted principally of inclusion of a rock density factor in 26.4b estimates and use of raw data with an assumed slope correction for the greater radial ranges in the 26.4a and 26.4e estimates. Castledale data and other close-in measurements of acceleration have established that, within one or two scaled radii, peak accelerations are degraded approximately as the inverse fourth power of distance, as predicted by point-source theory. More remote seismic observations and acceleration data show a degradation at more nearly an inverse square rate. The

transition region is shadowy and may involve either a gradual change or an unstable one. The transition seems to occur as the close-in predominance of the compressional wave, which decays rapidly, as r^{-4}, fades into the more remote predominance of the surface wave, which degrades more nearly as r^{-2}. This follows evidence that acceleration maxima, which constitute the initial signal at small radii, occur in later portions of the records at more remote instrumentation.

Set ranges for Project 26.4b accelerometers were derived from a family of empirical curves (Fig. 2.1) based on an equation giving scaled acceleration, $A\rho\lambda$, as a function of scaled radial distance, R/λ,[4]

where A is peak acceleration in g-units
ρ is bulk density or specific gravity of a gross volume (not particle density)
λ is the scale factor based on the cube root of the TNT energy equivalent in pounds (units are $ft/lb^{1/3}$)
R is the radial distance in feet.

The curve family includes curves for a material density of 1.6 and TNT energy equivalents of 100, 50, 25, and 10 percent of predicted radiochemical yield for the Rainier device.* Fifty percent of predicted yield was assumed, and set ranges were chosen accordingly. The curves in Fig. 2.1 include estimates used by Project 26.4b. No allowance was made for the change in attenuation rate with range, mentioned in the preceding paragraph.

Set ranges for strain measurements were determined primarily for anticipated maximum compression. For the gages near zero, out to 200 feet radial distance, 10-percent strain was assumed on the basis of estimated 30-percent voids in the material. Lower strain rates of 5 and 2.5 percent were estimated for the more remote gages.

*Predicted yield for Rainier was 1.8 kt. Actual yield published after the event was 1.7 kt. Consequently, set range prediction is based on 1.8 kt, data analysis on 1.7 kt.

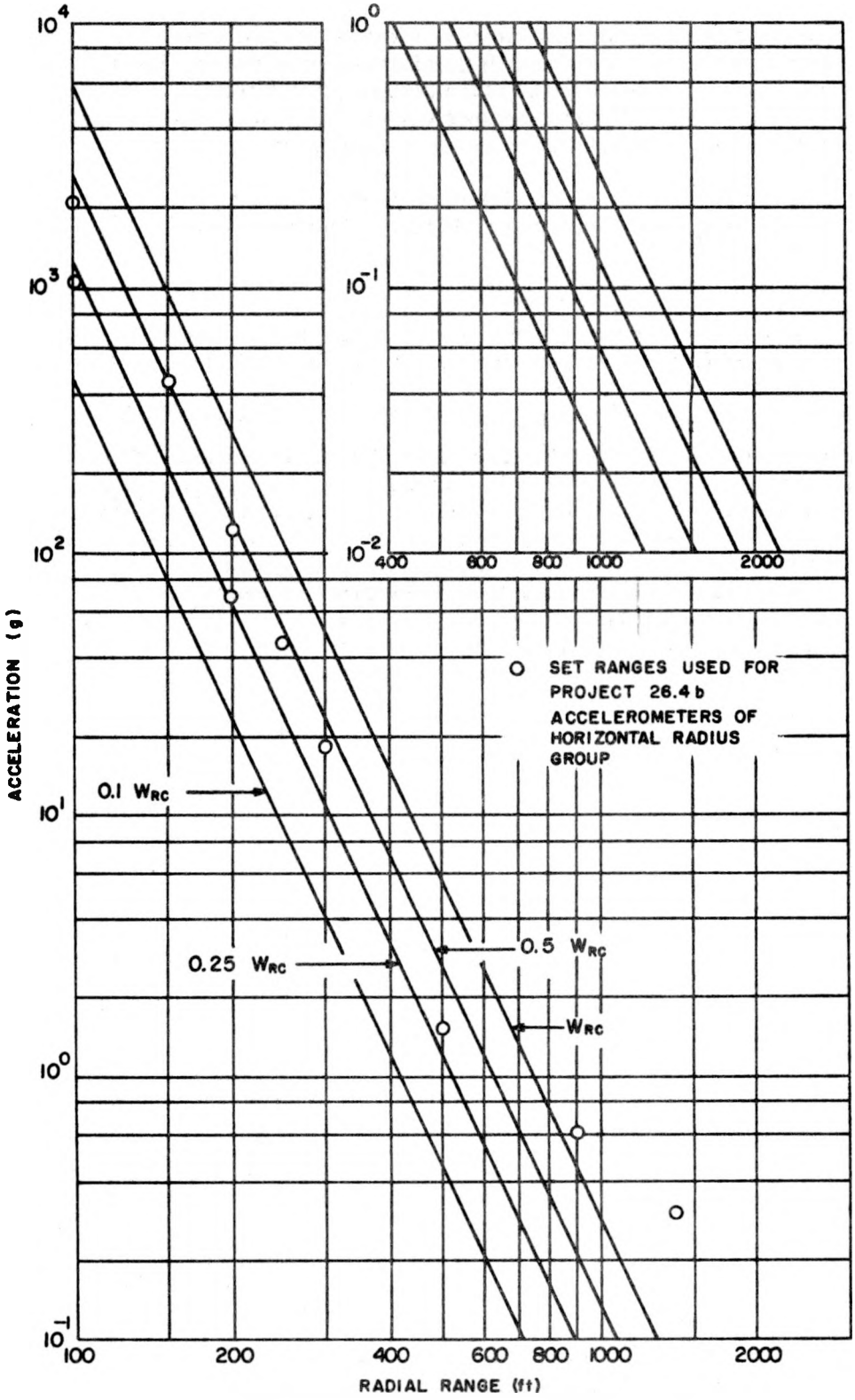

Fig. 2.1—Rainier prediction curves for acceleration.

Chapter 3

INSTRUMENTATION

3.1 GENERAL PLAN OF INSTRUMENTATION SYSTEM

Recording instrumentation for Project 26.4b was divided into two systems. One system, located at Station 12-26.4-6006 and serving the vertical instrument array, included a 22-channel amplifier-recorder package housed in a trailer located about 2,500 feet south and west of surface zero on the mesa. The other, including a similar amplifier-recorder package, was housed in a timbered portion of tunnel U-12-d near the main access tunnel (Fig. 1.2) and served the horizontal instrument array.

Instruments for the vertical-radius array were placed in a single 7-inch-diameter boring which, because of drilling difficulties, was terminated at a depth of 535 feet rather than at the planned depth of 800 feet. Signal cables from the gages were laid in a bundle from the instrument boring 25 feet south of surface zero to the recording trailer. The cable bundle was suspended in long catenaries between trees or other supports from which they were hung on loops of elastic shock cord (Fig. 3.1). Plank culverts protected cables from traffic damage at all roadway crossings.

Accelerometers in the tunnel array (horizontal radius) were placed in 6-inch-diameter holes beneath the tunnel floor. Relative displacement gages were placed within niches in the north wall above the floor. Signal cables were carried to the tunnel portal in one of a series of metal cope trays along the south wall of the tunnel. From the main tunnel portal the cables were run in the open beneath a massive overhanging rock ledge to the portal of the U-12-d recorder station.

Amplifier-recorder systems used at each Project 26.4b recording station included Consolidated Engineering Corporation, System D, 3-kc carrier-amplifier units. The rectified output from each channel was

Fig. 3.1—Signal cable suspension.

comprised a length of piano wire anchored to the rock at one end and wrapped at the other end over a 2-inch-diameter spool in the transducer unit. The spool was spring loaded to maintain tension in the wire. Rotation of the spool, which followed relative motion between the fixed anchor and the transducer, actuated a helical potentiometer.

3.3.1 Tunnel System Gages

Relative-displacement gages assigned to the tunnel array used transducer elements recovered from Project 1.5 installations in Frenchman Flat.[12] These gages were installed in shallow niches in the tunnel wall (Fig. 3.3). Transducer elements were located at the nominal radial distance.

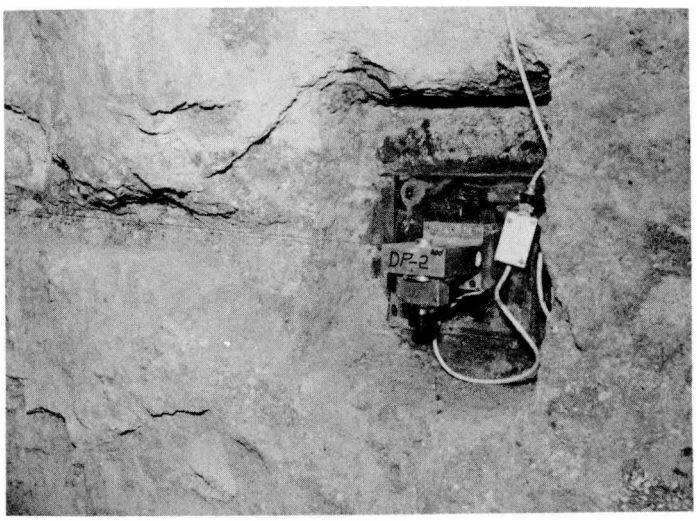

Fig. 3.3—Relative displacement gage transducer, tunnel wall mounting.

3.3.2 Vertical System Gages

Gages used to measure long-base strains in the vertical boring, and designed specifically for this project, were required to meet conditions imposed on an instrument array suspended on dual messenger cables in a vertical boring (Fig. 3.4). These gages are direct descendants of those used in the tunnel, but are more compact and waterproof. The transducer unit was attached to the messenger cables by clamps at each end. A length of corrugated bronze tubing, which enclosed the gage wire, was attached directly to the transducer case. The lower end of the flexible tubing was attached to a cross bar, also clamped to the messenger cable.

3.4 BLAST SWITCH AND CIRCUIT

Detonation of the Rainier shot in a tunnel posed a timing problem for effects measurement projects because precise zero-time signals could not be derived in the customary manner. Obviously, the usual dependence on a blue-box signal was not practicable. Uncertainties of

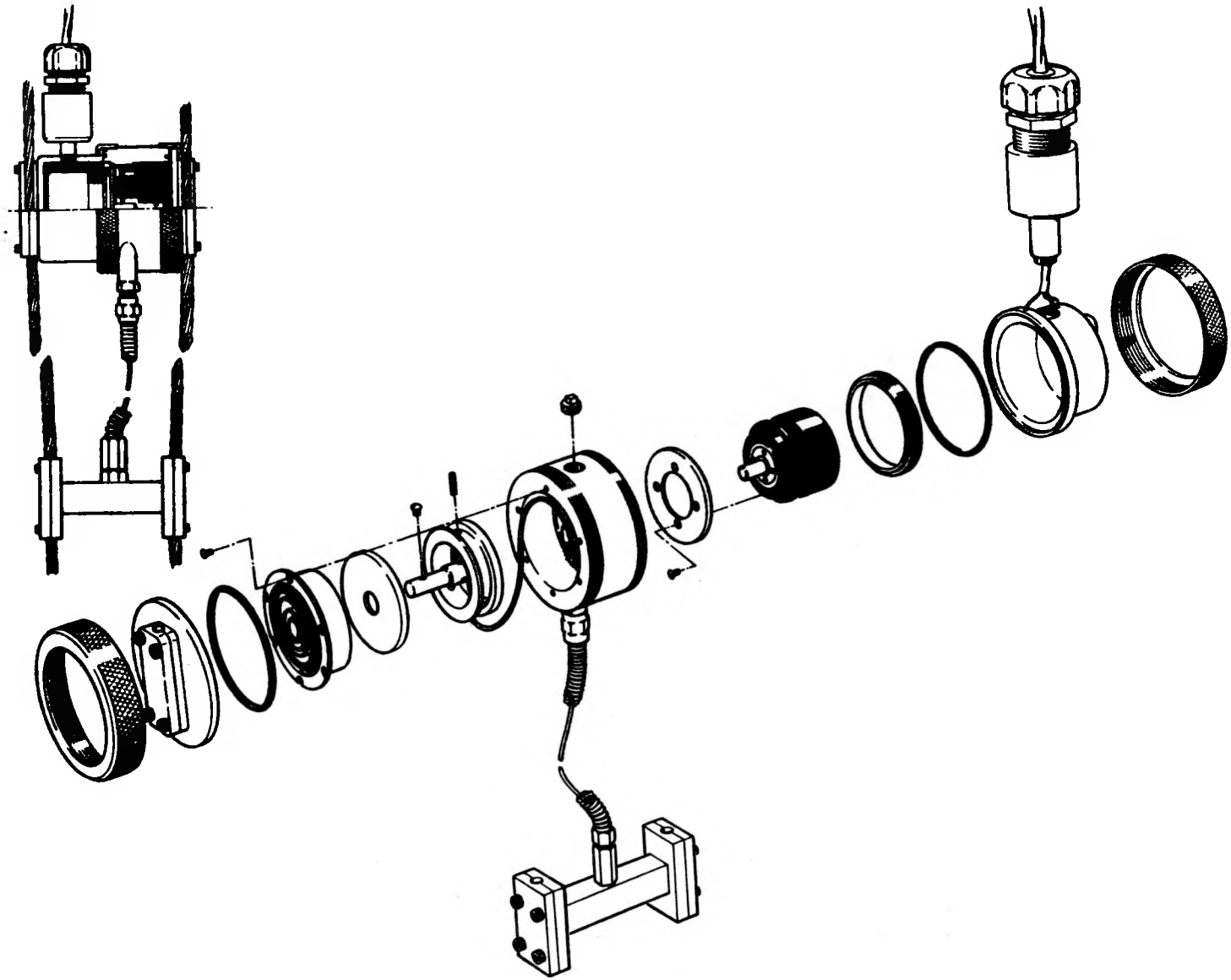

Fig. 3.4—Relative displacement gage for vertical hole.

the order of several milliseconds in closure time in the EG&G timing relays do not handicap their use as start-up timers, but do radically limit their usefulness for zero-time signals for recorded data at ranges less than 1,000 feet. Zero-time signals for certain projects were derived from elements of the fusing circuits of the device, but it was not considered advisable to include the strong motion projects of Program 26 in that zero-time circuit.

Consequently, a rough but effective blast switch, comprising two discs of 16-gauge copper sheet separated by a thin ring of micarta, was placed on the inner wall of the copper-lined detonation room. This normally open switch was connected in a series circuit with a battery and load resistor. A voltage signal from the load resistor was fed into the 250-cps timing channel at the Project 26.4b U-12-d recorder station. Originally, it was planned to carry the same zero-time signal to the recorder station for the vertical gage system on the mesa top, but ground loops caused malfunction of the circuit on dry-run tests. Therefore, the blast-switch time was supplied only to the U-12-d recorders, but the EG&G zero-time signal from a single relay was furnished to that recorder as well as to the recorders of the Project 26.4b mesa-top station and the Project 26.4e recorders. In order to ensure a zero-time tie-in with Project 26.4a, a second EG&G zero-time relay was used at the mesa-top recorder stations of Projects 26.4a and 26.4b. Thus, the true zero-time signal (blast switch) could be transposed to the records for all three projects by correction factors which were precise to 1 millisecond or better.

Chapter 4

INSTALLATION OF INSTRUMENTS

4.1 TUNNEL INSTRUMENTATION SYSTEM

The access tunnel for Rainier shot was mined approximately level into the mesa at 6,612 feet msl and included one section offset 20 feet northward. A spiral at the inner end placed zero for the device about 48 feet from the centerline of the main tunnel (Fig. 1.2). This tunnel geometry caused radially oriented gages at various ranges within the tunnel to be oriented at progressively greater angles to the tunnel certerline as ranges decreased. Conversely, gages attached to the tunnel wall, parallel to the centerline, made progressively greater angles with the radial direction at decreasing ranges.

4.1.1 Accelerometer Installation

Accelerometers in canisters with side-mounted orienting stubs were placed in holes in the tunnel floor. Holes within 300 feet of zero were filled with water, dirt, and small debris, and bailing was required immediately before the gages were placed.

Gage canisters were lowered into the holes and positioned by use of a Brunton compass to proper orientation. Gages were placed with an angular error of less than 5 degrees. Gage depths varied between about 8 and 11 feet, but errors caused by orientation and depth are probably in all cases less than 1 percent.

Grout composed of a high-early strength portland cement and low-density sand was pumped into each hole to a point about a foot above the gage canister. The orienting tube was removed a few minutes after the first grout was placed, and grouting was continued to the tunnel-floor level. A short length of half-inch reinforcing bar was placed vertically in the grout of each hole to serve as a marker for preshot and postshot displacement surveys.

4.1.2 Displacement Gage Mounting

Displacement gages were mounted on the north wall of the tunnel opposite the cable trays (Fig. 4.1). Transducer units were attached to steel plates lagged into the wall with 12-inch screws and expansion anchors. A thin layer of cement grout behind the plates ensured solid backing over the entire area of the plates. Gage wires were anchored to lag bolts set into the tunnel wall. Three of these gages covered 10-foot spans; the most remote gage, DP-4, covered a 20-foot span. Transducer units were placed, where feasible, adjacent to an accelerometer station, and the gage span extended down the tunnel toward zero. Wires between the transducer units and anchors were strung in shallow channels in the tunnel wall, and depths of transducer and anchor niches were adjusted so that the wires were free in the channels, yet did not project into the tunnel.

Displacement gage transducers at the three closer stations were located adjacent to accelerometer stations as planned. The assigned position for the fourth gage, DP-4, at 500-foot range, occurred in the diagonal tunnel offset. Since this position would have caused the gage to be oriented about 50 degrees off radial, the gage was moved around the tunnel bend toward zero, where the angular departure from radial was only 6 degrees. The transducer of DP-4 was installed at Station 12+50 at radial range 429 feet.

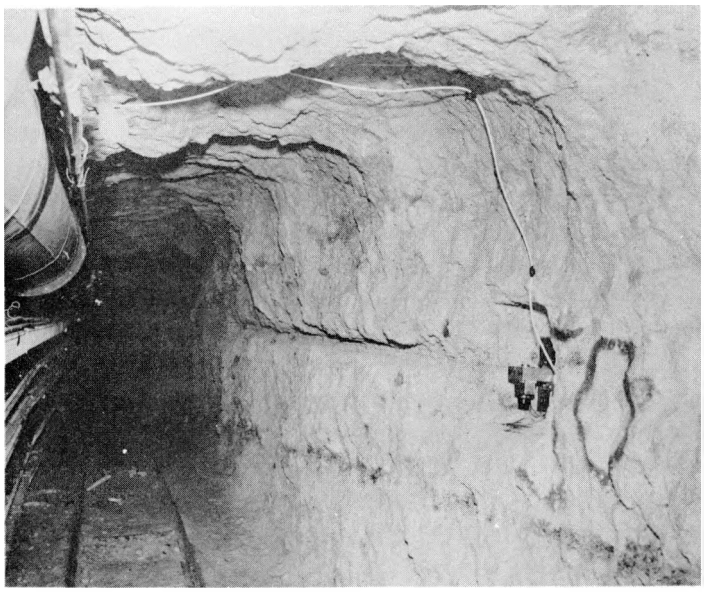

Fig. 4.1—Relative displacement gage on tunnel wall.

4.1.3 Three-Component Acceleration Measurement

One instrument station was established within the mesa close to the outer slope at the Sandia recording tunnel, U-12-d. This station was located adjacent to USC&GS strong motion Station 05 to provide for comparison of data from the two measurement systems. Both stations were instrumented to observe three components of acceleration: vertical, radial, and tangential. The radial range of these stations was about 1,350 feet, the USC&GS station being about 14 feet closer to zero than the Project 26.4b one.

Gages used for the Project 26.4b station were low-range Wiancko accelerometers mounted in a steel canister of the type used for similar three-component measurements during Operation Upshot-Knothole.[13] The canister was grouted into a shallow hole in the tunnel floor.

4.2 VERTICAL-BORING SYSTEM

The gage array for the vertical-radius instrumentation was to extend from a point 100 feet above the Rainier device to the mesa top near surface zero. Difficulties encountered in drilling restricted the deepest hole available for vertical instrumentation to a depth of 535 feet, approximately 361 feet above zero elevation. Subsequently, the instrument plan was altered to cover this region, and duplicate gages were used at several levels to provide

back-up. Figure 4.2 shows the plan projection of the 26.4b instrument boring. Departures from vertical produced errors in observed acceleration of less than 1 percent.

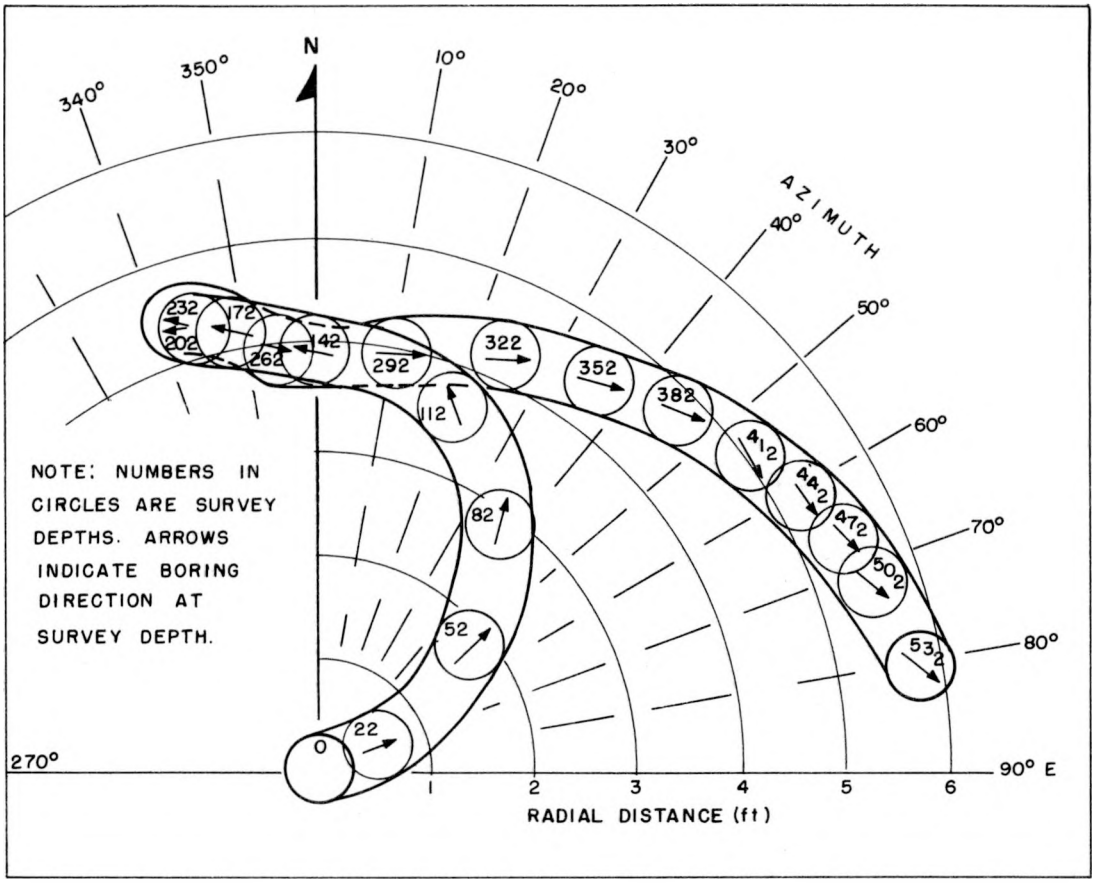

Fig. 4.2—Plan projection of vertical hole.

4.2.1 Assembly and Installation of Vertical-Gage Array

Thirteen gages, including eight accelerometers, three relative-displacement gages, and two temperature-sensing elements (Project 26.3) constituted the vertical array. Each of these gages required 3- or 4-conductor signal cable, and the grouting procedure, discussed later, required the presence of from one to four 1-inch-ID plastic hoses. Individual placement of the gages would have presented unnecessary complications even in a straight vertical hole. The more serious difficulties to be encountered in lowering individual instruments past signal cables and grout hoses in a crooked hole (Fig. 4.2) could be anticipated. Therefore, continuous assembly of the entire array on a pair of messenger cables, lowered into the borings as assembly progressed, eliminated such difficulties.

Two quarter-inch steel aircraft cables—one right-lay, the other left-lay—were wound on separate reels attached to a common shaft. These 600-foot cables were stretched into the hole under a 50-pound weight and flagged with tape at 50-foot intervals under tension to provide

a scale for attaching instruments. The counter-lay of the cables minimized twist in the instrument assembly, a condition desirable for the long-span displacement gages, but not particularly important for the other gages. Twin cables with gages secured between them also provided more effective isolation of the displacement-gage wire and surrounding flexible tubing within the grout.

Messenger-cable reels were mounted on a light jury-rigged A-frame, with a 30-to-1 worm-gear box driven through a 1/2-inch power drill equipped with a reversing switch (Fig. 4.3). This frame was set up about 35 feet from the instrument boring, over which two snatch blocks were rigged on a boom about 10 feet aboveground. Cables from the reels were run through the snatch block and downward into the hole. A 50-pound weight fixed at the cable ends held them taut during early stages of assembly when the weight of instruments and signal cables was small.

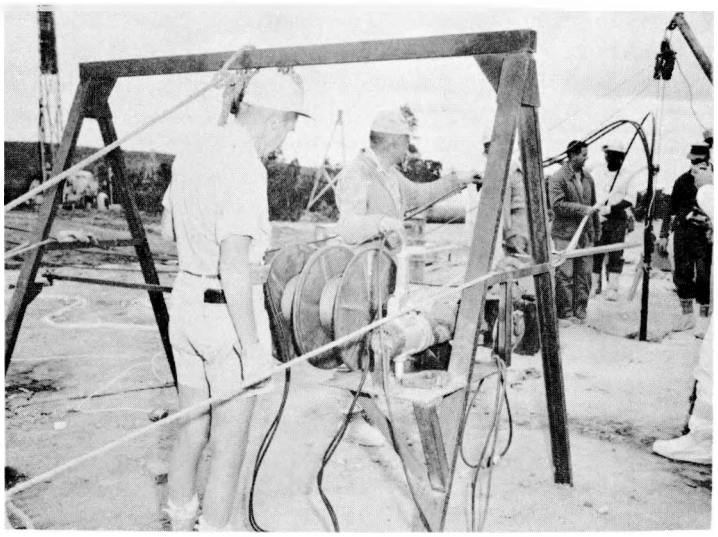

Fig. 4.3—Hoist and controls for vertical instrument array.

Accelerometer canisters were attached between the cables at prescribed positions. Signal cables from the gages were secured to the messenger cables with tape at intervals of about 15 feet. Relative-displacement gages were attached with the anchor ends of the wires on steel crossbars clamped to the cables at prescribed distance (10 or 20 feet) below the transducer units (Figs. 3.4 and 4.4). Two temperature gages, TS-1 and TS-2, supplied by Project 26.3, were attached to one messenger cable at radial ranges of 400 and 600 feet. Four grout hoses, terminating at depths of 485, 375, 250, and 100 feet, were attached by tape to the cable array during the lowering operation.

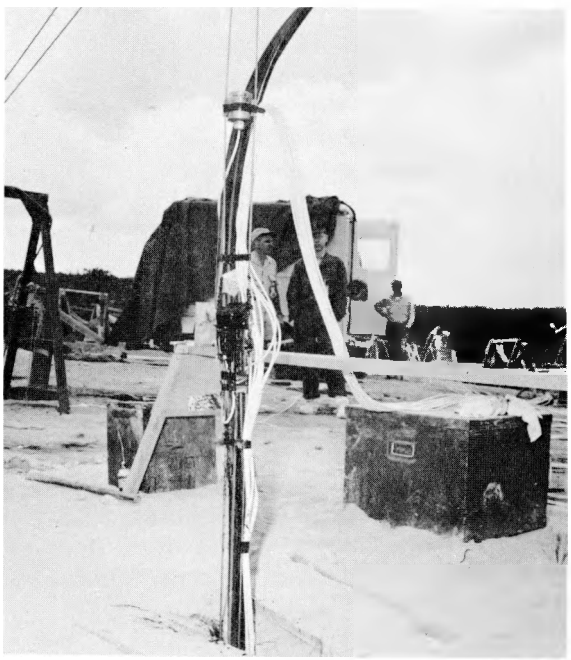

Fig. 4.4—Part of vertical instrument assembly.

4.3 DEEP-BORING GROUTING PROCEDURE

A special grout for use in Oak Spring tuff was devised by the Concrete Research Division of the Waterways Experiment Station (WES) at the request of Program 26. This grout imbedded instruments in the

deep vertical holes in a material of density, modulus, and strength roughly similar to the surrounding rock. The grout was designed to provide, after a 14-day curing period, a slight mismatch to the Oak Spring tuff, in the direction of lower seismic velocity (lower modulus) and lower strength, so that the motion and compression of the large mass of the surrounding rock would control response of the instruments and minimize perturbation introduced by the instrument boring.

All grouting operations were performed under the direction of Mr. James Polatty, of WES, who designed and tested the grout. Batches of grout, consisting of 9.5 percent Type III cement, 61.6 percent expanded shale sand, 22.0 percent water, and 6.3 percent diatomite, by weight, were mixed and pumped through the 1-inch-ID plastic hose which had been lowered with the instrument array. All accelerometer channels of the Project 26.4b vertical system were monitored during grouting. Each channel showed agitation of its end instrument by grout until it became submerged. Quiescence of successively shallower gages showed progress of grouting up-hole. As the operation progressed, hoses terminating at successively shallower depths were used, as appreciable back pressure was developed by grout in the boring above the end of the deeper hose.

Grouting progressed smoothly during the entire operation. Assembly of the instrument string was started at about 1030 hours on D-2, and the instruments were ready for grouting by 1400. Grouting in the Project 26.4b boring was completed shortly before midnight of the same day.

Test cylinders of the grout were made during pumping operations in the two instrument borings, Projects 26.4a and 26.4b. These cylinders were tested after they had aged for 4 days. Average data from the cylinders are compared with data from rock cores from an adjacent boring in Table 4.1.

TABLE 4.1—COMPARISON OF AVERAGE PHYSICAL PROPERTIES OF GROUT AND OAK SPRING TUFF

Parameter	Grout	Oak Spring tuff
Specific gravity	1.596	1.4 - 1.9
Velocity (ft/sec)	4600	3000 - 7000
Dynamic modulus (psi)	23×10^4	$8\text{-}20 \times 10^6$
Static modulus (psi)	17×10^4	$6\text{-}15 \times 10^6$
Strength (psi)	97	2000 - 8600

Since Rainier was detonated about 48 hours after completion of grouting in the Project 26.4a boring and 36 hours after completion of the Project 26.4b boring, the observed moduli and strength for the test cylinders are probably greater than those for the grout surrounding the instruments at shot time. However, these differences are not considered sufficient to affect performance of the installation adversely, and the mismatch between properties of the grout and rock was still acceptable.

Chapter 5

DATA

5.1 RECOVERY

Containment of Rainier was complete, and recovery of records from both Project 26.4b recorder stations was feasible within a few hours after shot time. All information channels and tape transports operated normally. Postshot checks showed normal circuit resistance and insulation from ground for all channels except those nearest zero in the tunnel. Signal cables from all instruments within 300 feet of zero in the tunnel were damaged.

A cursory survey of the surface area showed little disturbance other than that three of the cable-support horses had tipped over about 300 feet from surface zero (Fig. 5.1), one crack had developed adjacent to the Project 26.4b boring (Fig. 5.2), and numerous cracks were opened (Fig. 5.3) within 200 feet of surface zero. The largest ones, near surface zero, showed a spread of about 2 inches and residual vertical displacements of 2 to 3 inches. It was not evident from this survey which cracks included fresh breaks in the cap rock, but, certainly, many of them included portions of joints observed on the surface before the shot.

5.2 PLAYBACK

Magnetic tape records required playback for analysis. The playback system used for this purpose includes a compensator circuit for wow and flutter derived from high speed operation of the recorder tape transports. Playback is limited to a timing trace and a single information channel on each oscillograph record. Flexibility of the system permits records to be made within a wide range of both time and amplitude scales to facilitate analysis or reproduction.

5.3 ZERO-TIME RECORDINGS

Satisfactory performance of the blast switch circuit is demonstrated by coincidence of its signal on the 250-cps timing trace and small zero-time transients on some of the traces from gages close to the burst. Reduction of the timing-channel data shows that the EG&G zero-time relay signal at the U-12-d recording station lagged the blast switch by about 27 milliseconds. The EG&G zero-time relay signal at the mesa-top recording trailer, Station 12-26.4-6006, led the U-12-d relay signal by about 3.5 milliseconds. Precise times as read on a comparator are:

Tunnel	Mesa
Blast Switch: 0.0 milliseconds	U-12-d EG&G Relay: +28.0 milliseconds
U-12-d EG&G Relay: +27.3 milliseconds	Sta. 12-26.4-6006 EG&G Relay: +24.5 milliseconds

Fig. 5.1—Postshot condition near surface zero.

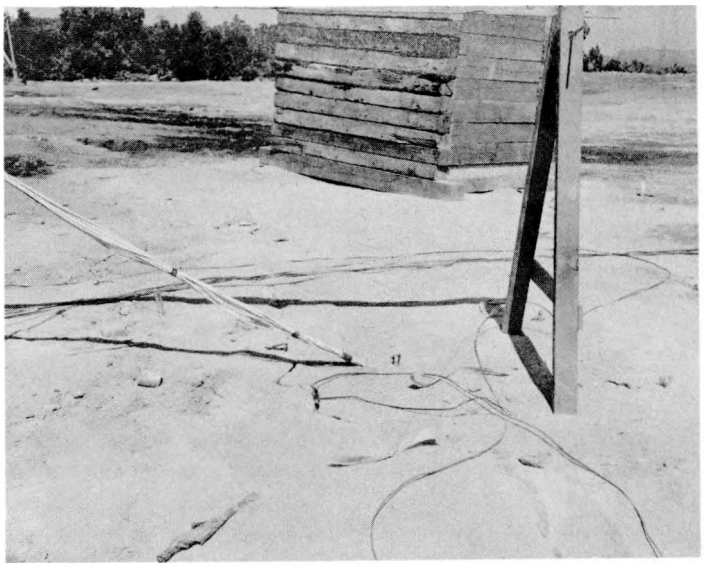

Fig. 5.2—Crack near Project 26.4b vertical hole, postshot.

Fig. 5.3—Surface crack near zero, postshot.

Project 26.3 thermometers at 400 and 600 feet from zero on the 26.4b vertical radius received a transient signal at zero time which, although apparently meaningless as a temperature indication, is useful as a means for correlating times. These signals were used for fixing the timing-relay delays at the mesa recording station. The 0.7-millisecond lead of the U-12-d relay timing signals over the relay signal on the mesa is probably consistent with closure-time differences for different sets of contacts on the same relay. It is about 10 times the computed delay of the line which transmitted the signal between stations.

5.4 TUNNEL RECORDS

Records from tunnel gages of Project 26.4b were of relatively short duration because of proximity of most gages to the explosion. Signal cables from all gages within a 300-foot radial range were damaged within about 60 milliseconds after detonation. This did not affect early parts of the acceleration records adversely, but limited their useful duration. The accelerometer record from AHP-5 at 300-foot radial range showed no perturbation until about 360 milliseconds after detonation. Accelerometer records from stations at 500- and 900-foot radial ranges and from the gages in the U-12-d recording station were not limited in time.

Records from relative displacement gages on the tunnel walls were limited to very short and generally insignificant signals. Cables from all of these gages were damaged. At short radial ranges, gages recorded only the early portion of motion before cable damage or spalling rock rendered them meaningless. Gages at ranges out to 300 feet gave records legible to between 50 and 100 milliseconds; the record for DP-4 at 424 feet shows no major perturbation.

Data derived from preliminary studies of acceleration records from the horizontal radius gages are assembled in Table 5.1. Similar data from the strain or relative displacement gages on the horizontal radius are included with those for vertical radius in Table 5.2. These data are reasonably good interpretations of the records but may be expanded and altered during more thorough analysis for the final report. Acceleration versus time records for the horizontal radius gages are shown in Figs. 5.4 through 5.6. Relative displacement versus time curves are presented in Fig. 5.7.

5.5 VERTICAL-BORING RECORDS

Records from all vertical-radius gages show no limitation such as that caused by cable damage in the tunnel. However, DS-2, a displacement gage which was terminated near the interface between the rhyolite cap rock and underlying tuff shows a marked perturbation, caused by an FM oscillator malfunction, at about 500 milliseconds after zero time. Data derived from preliminary studies of the vertical acceleration records are presented in Table 5.3 and data from the vertical-radius relative-displacement gages are in Table 5.2. Acceleration-time records from the vertical-radius gages are included in Fig. 5.8 and the vertical relative displacement versus time data in Fig. 5.9.

Data quoted in Table 5.3 and plotted in Fig. 5.8 include corrections to the records from the four shallowest gages, AVS-3, AVS-4, AVS-5, and AVS-6. The nature of these records, broad flat-topped upward peaks at about 2 to 2.5 times set range, showed obvious overranging and characteristics distinctly different from those of records from corresponding gages of the SRI (Project 26.4a) installation. It is obvious that integration of the raw data from the shallower AVS gages would lead to spurious velocity and displacement data and would yield useless results. The AVS records were not shortened by cable breaks as were some of the SRI data, so an effort to operate on the AVS records biased by applicable SRI results seemed worthwhile. Corrections to the shallow AVS records consisted of: (1) manual adjustment of AVS-6 and AVS-5 to agreement of peak values with corresponding peaks in SRI records and (2) digital computer corrections using factors derived from plots of positive and negative peak data from

AVS-5 and AVS-6 versus the corresponding SRI data. In general, machine corrections were satisfactory for the flat negative portion of the record (free-fall), but were too gross for the high positive peaks. The latter condition stems from the extremely poor recorder sensitivity in the region of amplifier saturation and the consequent lack of refinement in the corrected curve. Dashed curves for AVS-6 and AVS-3 in Fig. 5.8 are manual corrections (solid lines are raw data); dashed curves for AVS-5 and AVS-4 are machine corrections.

5.6 DISCUSSION OF RAW DATA

Relatively short useful spans of the records from the Project 26.4b instruments nearest the detonation were anticipated. However, a more serious restriction on usefulness of many of the records from this project is the considerable overranging to which gages were subjected. All gages were calibrated to 4/3 of set range to derive useful information from incident events as much as 33 percent greater than estimated. Response of most recording channels was linear over the full calibrated range; although, in a few, minor nonlinearity became evident between set range and 4/3 set range. The serious restriction on the Project 26.4b data lies in the channels, generally those for the more remote gages, which were loaded above set range by factors between 2 and 10. The extent of this overranging is indicated by the character of the records or by nearby gages of other projects.

Many of the accelerometers used in Project 26.4b were designed to give nearly linear response for peak accelerations 2 or 3 times the estimated set range for their station. However, optimum performance of the carrier-amplifier system near set range and acceptable signal-to-noise ratio at lower signal amplitudes usually result in increasingly nonlinear response beyond set range. This saturation effect becomes serious when the input signal becomes 2 or 3 times set range. Consequently, precision of badly overranged channels drops off radically at the peaks, although it may remain better than 10 percent for other portions of the record.

TABLE 5.1—PROJECT 26.4b ACCELERATION DATA - HORIZONTAL RADIUS

Gage	Range (ft)	Arrival time (msec)	Outward peak (g)	Inward peak (g)	Set range (g)
AHP-1	99	3.76	2550	3550	2100
AHP-1X	99	8.14	3120	2190	1050
AHP-2	148	12.1	1510	1490	450
AHP-3	199	19.6	242	260	120
AHP-3X	199	20.7	191	126	66
AHP-4	250	25.4	101	66.1	45
AHP-5	300	30.4	41.2	72.5	18
AHP-6	501	57	1.49*	3.28	1.5
AHP-7	901	122	1.34	0.90	0.6
AV	1355	186	0.67	0.66	0.3
AR	1355	180	0.55	0.56	0.3
AN	1355	190	0.55	0.51	0.3

*This peak was clipped in playback; deterioration of the tape prevents further playback of this channel.

TABLE 5.2—PROJECT 26.4b - STRAIN DATA

Gage	Range* (ft)	Span (in.)	Arrival time (msec)	Peak positive displ.** (in.)	Peak negative displ. (in.)	Max. positive strain (%)	Max. negative strain (%)	End of record (msec)
Horizontal Radius								
DP-1	151	120	11.9	0.87	-	0.73	-	23
DP-2	199	120	26.3	1.79	0.30	1.49	0.25	77
DP-3	300	120	37.4	0.81	-	0.68	-	58
DP-4	424	240	50.6	0.88	-	0.37	-	132
Vertical Radius								
DS-1	381	120	59	0.17	0.16	0.14	0.13	2508
DS-2	683	120	104	0.07	0.02	0.06	0.02	504
DS-3	696	240	100	0.14	0.26	0.06	0.11	2588

*Range gives radial distance from burst point to upper end of gage span for vertical-radius gages and to outer end of gage span for horizontal radius gages.

**Positive values refer to upward displacement for vertical radius gages and outward displacement for horizontal radius gages.

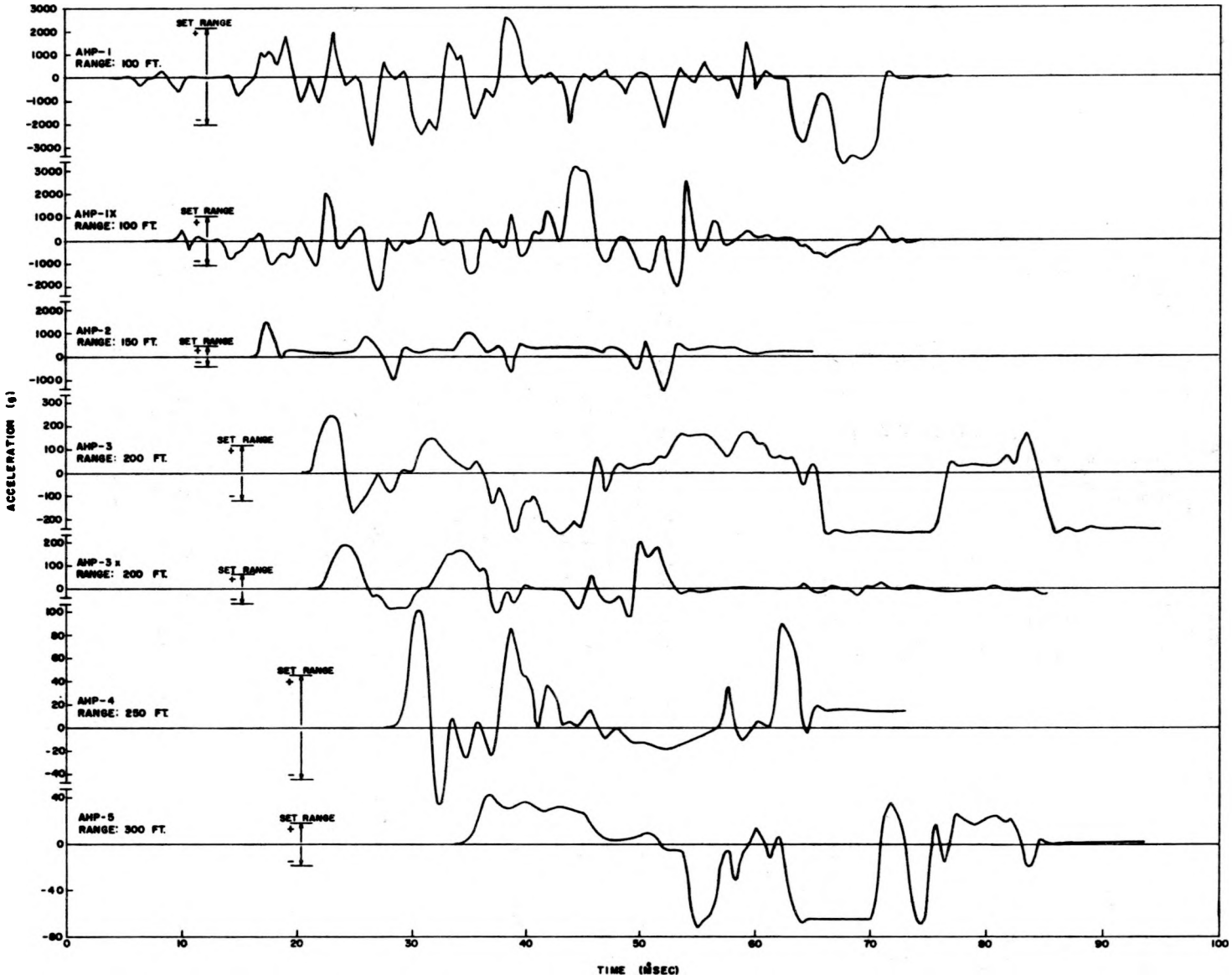

Fig. 5.4—Acceleration-time records, horizontal radius.

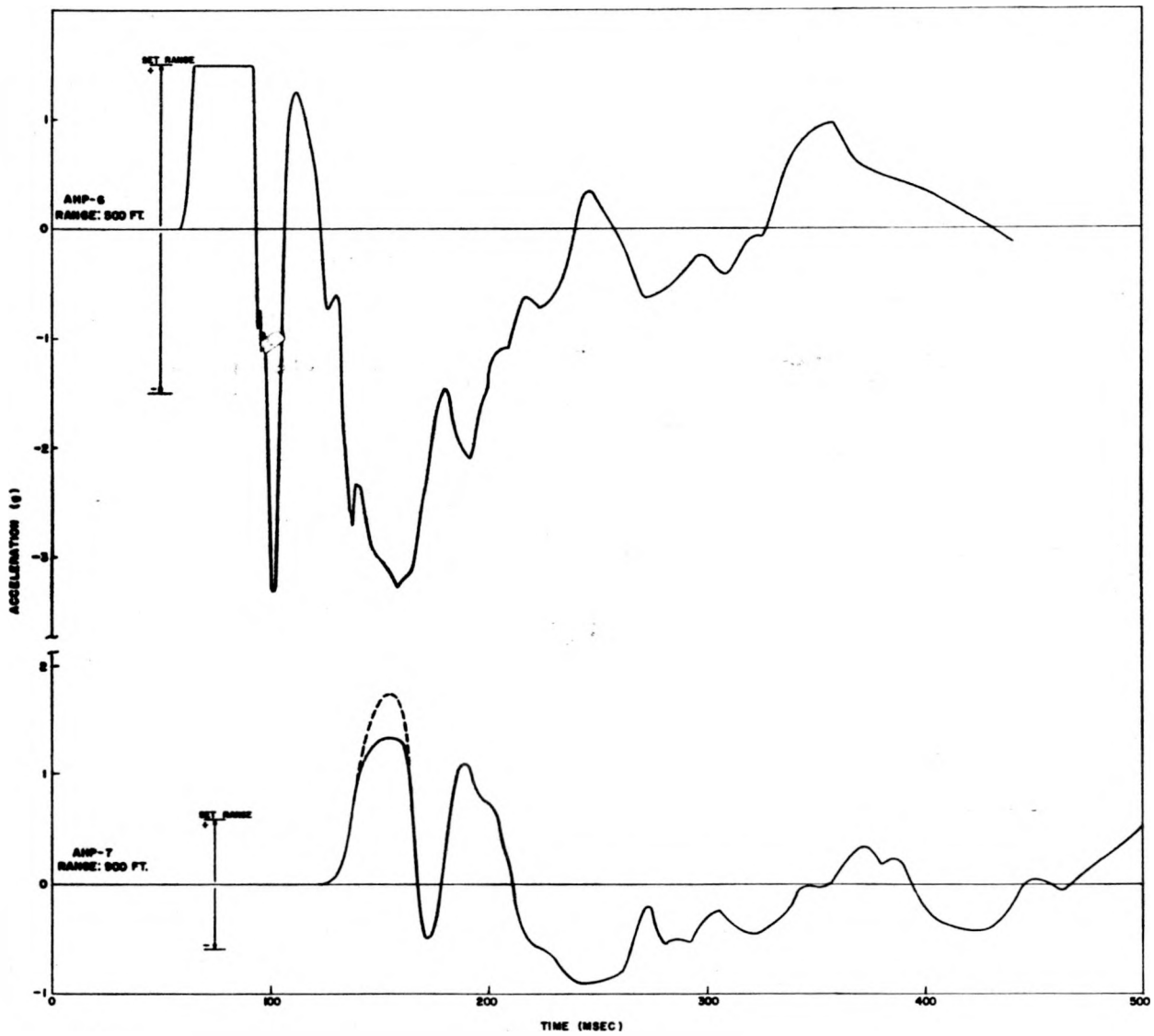

Fig. 5.5—Acceleration-time records, horizontal radius.

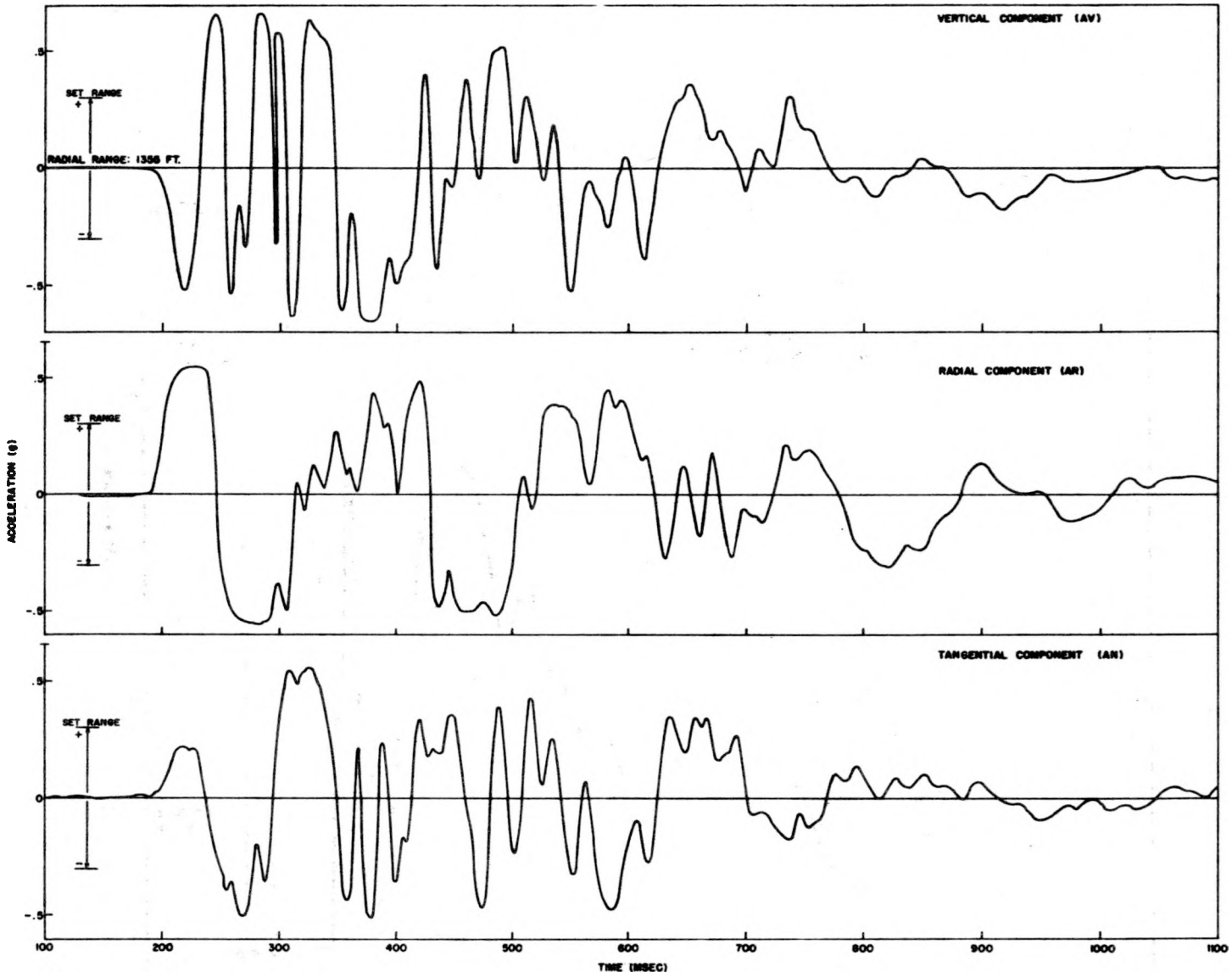

Fig. 5.6—Acceleration-time records, three-component station, Tunnel U-12-d.

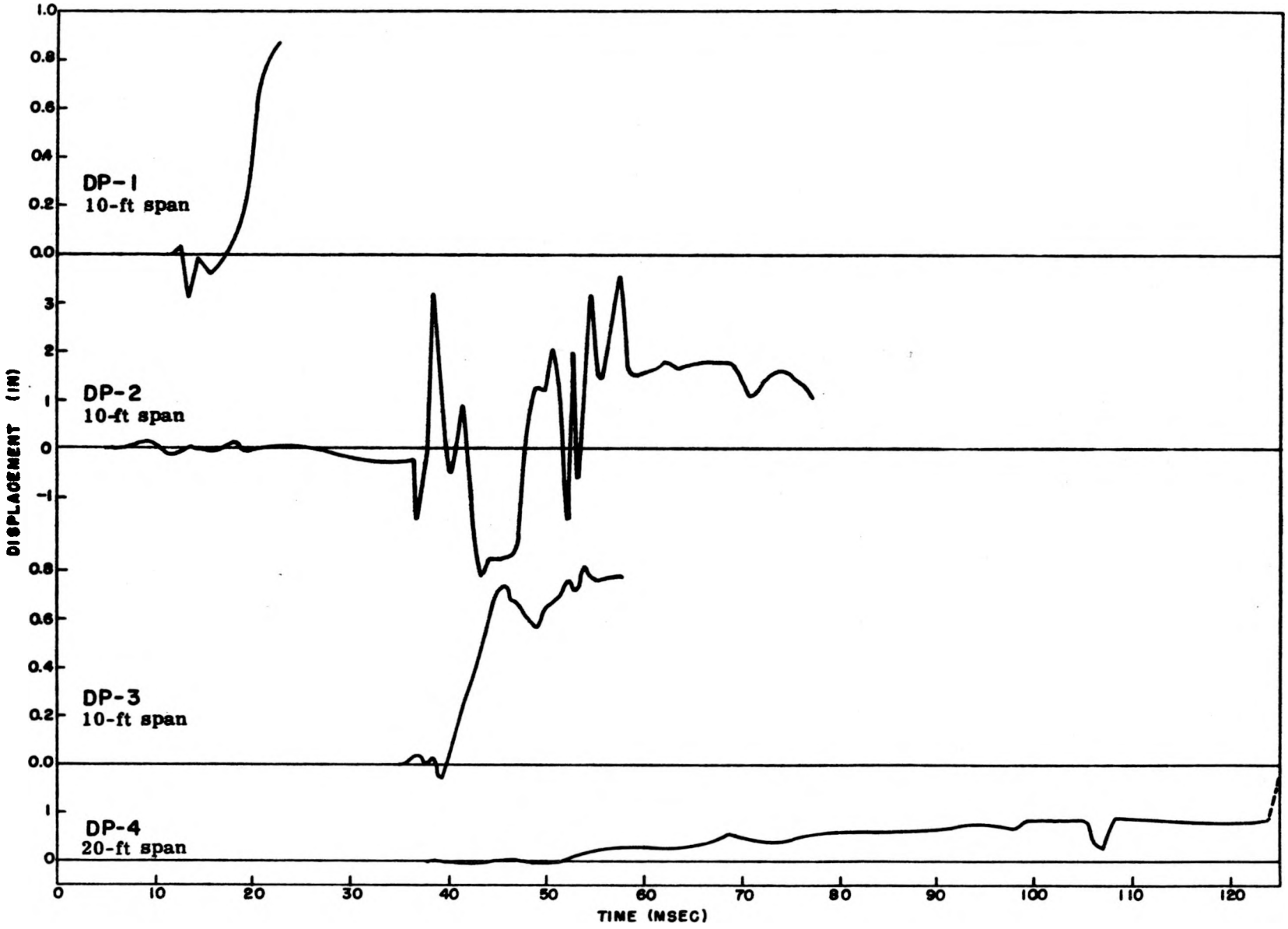

Fig. 5.7—Relative displacement-time records, horizontal radius.

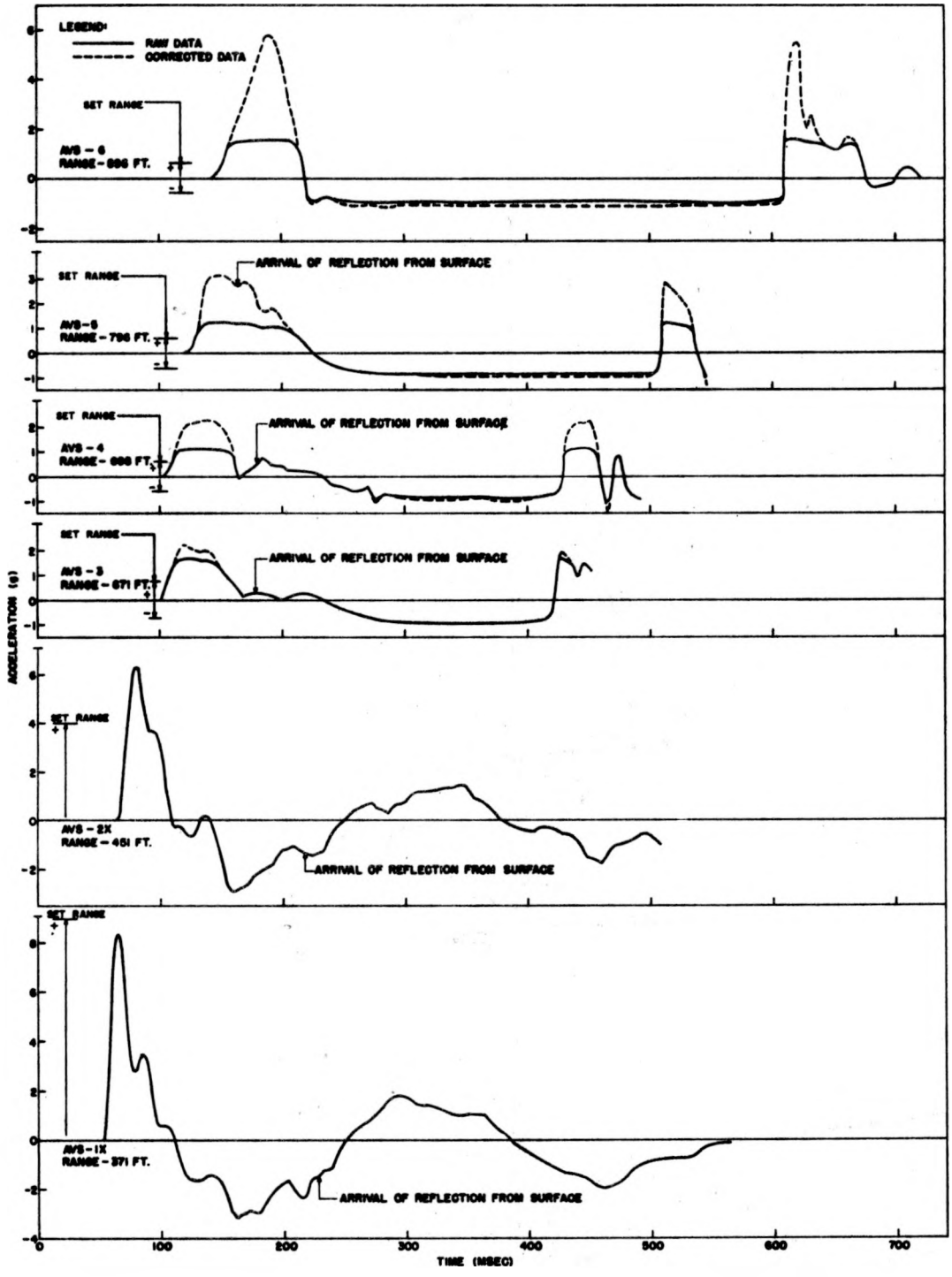

Fig. 5.8—Acceleration-time records, vertical radius.

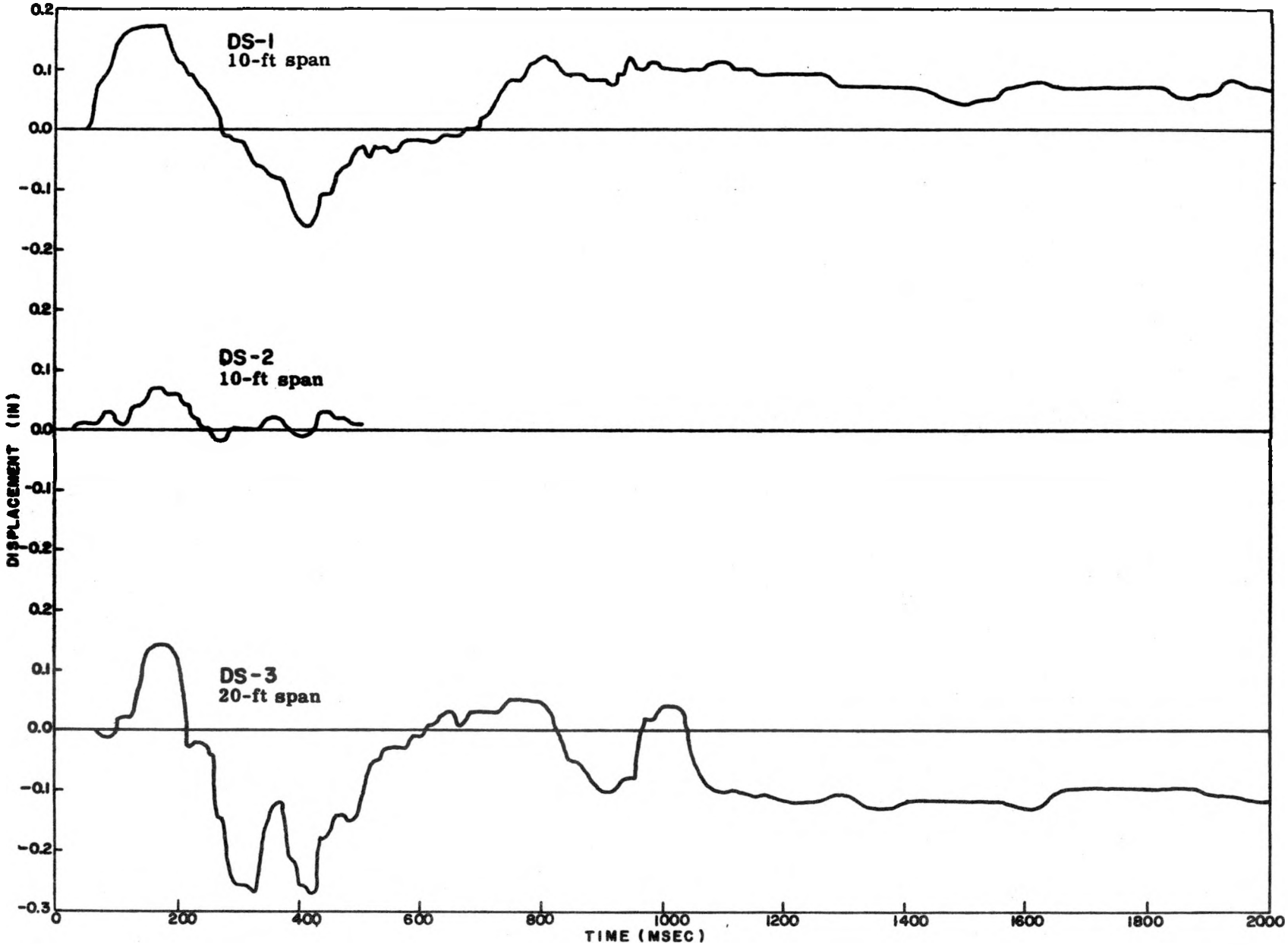

Fig. 5.9—Relative displacement-time records, vertical radius.

TABLE 5.3—PROJECT 26.4b ACCELERATION DATA - VERTICAL RADIUS

Gage	Range (ft)	Arrival time (msec)	Initial upward peak (g)	Peak-up time (msec)	Arrival of downward reflection* (msec)	Second peak-up time (msec)	Downward peak (g)	Start of levitation (msec)	Rebound time (msec)	Rebound peak (g)	Duration -1 g free fall (msec)	Set range (g)
AVS-1	366	53.4	8.02	65	227	85	2.88	-	-	-	-	6
AVS-1X	371	54	8.34	66	226	86	3.21	-	-	-	-	9
AVS-2	446	63.4	5.29	77	217	94 135	2.89	-	-	-	-	3
AVS-2X	451	64	6.28	80	216	94 138	2.91	-	-	-	-	4
AVS-3	671	101	1.67 (2.28)	121	179	172	0.98 (0.98)	278	412	1.69 (1.98)	134	0.75
AVS-4	698	104	1.13 (2.27)	144	176	185	0.93 (1.08)	275	414	1.13 (2.28)	139	0.6
AVS-5	796	118	1.23 (3.15)	152	162	198	0.88 (0.99)	272	506	1.20 (2.86)	234	0.6
AVS-6	896	140	1.54 (5.82)	191	-	236	0.94 (1.09)	250	609	1.50 (5.93)	359	0.6

NOTE: Numbers in parentheses are values derived by correction based on comparison of AVS-6 with corresponding SRI surface gage.

*Reflection arrivals are computed from observed interval velocities (Table 6.1) and are marked on Fig. 5.8.

Chapter 6

RESULTS

6.1 ANALYSIS OF TRAVEL TIMES

Arrival times derived from accelerometer records are generally readily discernible and significant within the limits of the recording system and timing devices. Arrival times indicated by displacement gages are less precise because of the longer rise times and slower initial rise of the displacement function.

Accelerometer arrival times and intergage intervals which represent the time required for shock motion to travel from the point of detonation to the nearest gage and between gages for both horizontal and vertical radii are presented in Table 6.1, together with derived propagation velocities. Two additional arrival times from Project 26.3 thermometers (TP-1 and TP-2) at 25- and 50-foot radial ranges in the tunnel wall are included. Arrival times for horizontal-radius gages are plotted versus range in Fig. 6.1; a similar plot for vertical-radius gages is included in Fig. 6.2. Slopes of the curves represent reciprocal velocities which appear to be roughly similar except in the region very near zero. Arrival times for vertical-radius gages occur about 10 milliseconds later than those for the horizontal array, suggesting rock of lower velocity directly above the burst than that along the access tunnel.

Propagation velocities (Table 6.1) are computed for the interval between the burst point and nearest gage and for intervals between gages. A rough estimate of error has been included in the tabulated range and time intervals. Range-interval-error estimates may be a little pessimistic with the exception of that for AVS-1, the range of which is subject to much more uncertainty than any of the other intervals. Time-interval errors are based on an assumed reading uncertainty of about 0.1 millisecond. The estimated errors for the two gages nearest the burst point take into consideration an expected greater error in defining zero time. All other time intervals are reckoned as differences between times read from the same zero time index. Velocities represent averages over the interval between gages. True velocities at specific points cannot be derived from data of the type included in Table 6.1.

Average propagation velocities derived for intervals along the horizontal radius are plotted in Fig. 6.3 as a function of radial range. The range of uncertainties is indicated by stippled areas. The high velocities at short ranges are associated with transmission of shock as compared with velocities in the seismic range for Oak Spring tuff at radii greater than 300 feet. The data suggest that energy transmission approached seismic velocities as close as 150 feet.

The similar plot of vertical velocities, Fig. 6.4, indicates velocities in the seismic range for Oak Spring tuff from the closest gage, at 366 feet, upward to the surface. The very broad band of uncertainty for the intervals near 370 and 450 feet are caused by the short (5-foot) interval between gages, and consequent emphasis on estimated errors. More significant is the indication of a high-velocity zone between 670 and 700 feet, which probably includes the

TABLE 6.1—PROJECT 26.4b - PROPAGATION VELOCITY DATA

Gage	Range (ft)	Arrival time (msec)	Range interval (ft)	Time interval (msec)	Propagation velocity (ft/sec)
			Horizontal Radius		
TP-1*	25	1.74	25±1	1.74±0.4	14,400±4,100
TP-2*	50	3.29	25±1	1.55±0.2	16,100±3,200
AHP-1X	99	8.14	49±1	4.85±0.2	10,100±600
AHP-2	148	12.1	49±1	3.96±0.2	12,400±900
AHP-3	199	19.6	51±1	7.5±0.2	6,800±300
AHP-4	250	25.4	51±1	5.8±0.2	8,800±500
AHP-5	300	30.4	50±1	5.0±0.2	10,000±600
AHP-6	501	57	201±3	26.6±0.2	7,550±200
AHP-7	901	122	400±4	65±0.2	6,150±100
AV*	1355	186	454±4	64±0.2	7,100±100
			Vertical Radius		
AVS-1	366	53.4	366±5	53.4±1.0	6,870±230
AVS-1X	371	54.0	5±0.5	0.6±0.2	8,330±4,000
AVS-2	446	63.4	75±1	9.4±0.2	7,980±250
AVS-2X	451	64.0	5±0.5	0.6±0.2	8,330±4,000
AVS-3	671	101	220±2	37±0.2	5,950±100
AVS-4	698	104	27±1	3±0.2	9,000±900
AVS-5	796	118	100±1	14±0.2	7,150±170
AVS-6	896	140	100±1	22±0.2	4,550±90

*TP = Gages are Project 26.3 temperature probes; AV = vertical accelerometer at U-12-d station.

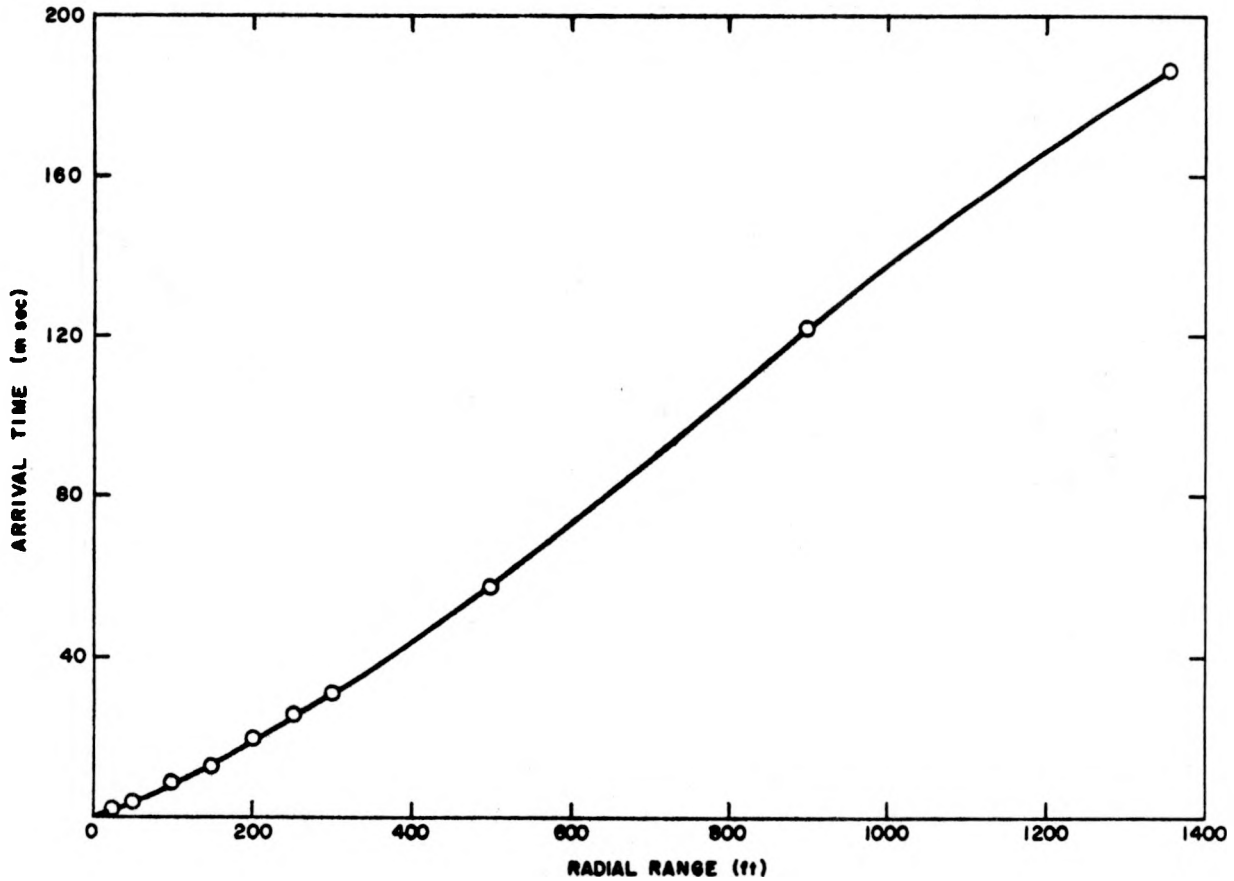

Fig. 6.1—Arrival time-range curve, horizontal radius.

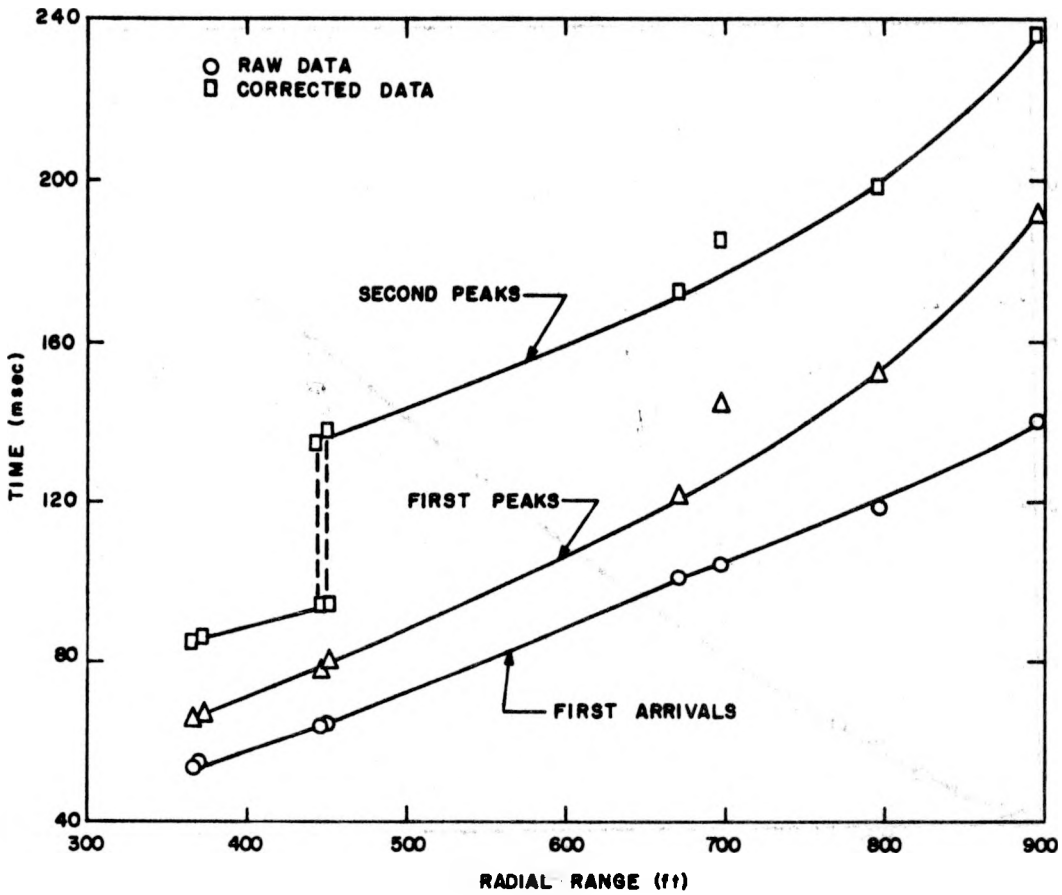

Fig. 6.2—Arrival time-range curve, vertical radius.

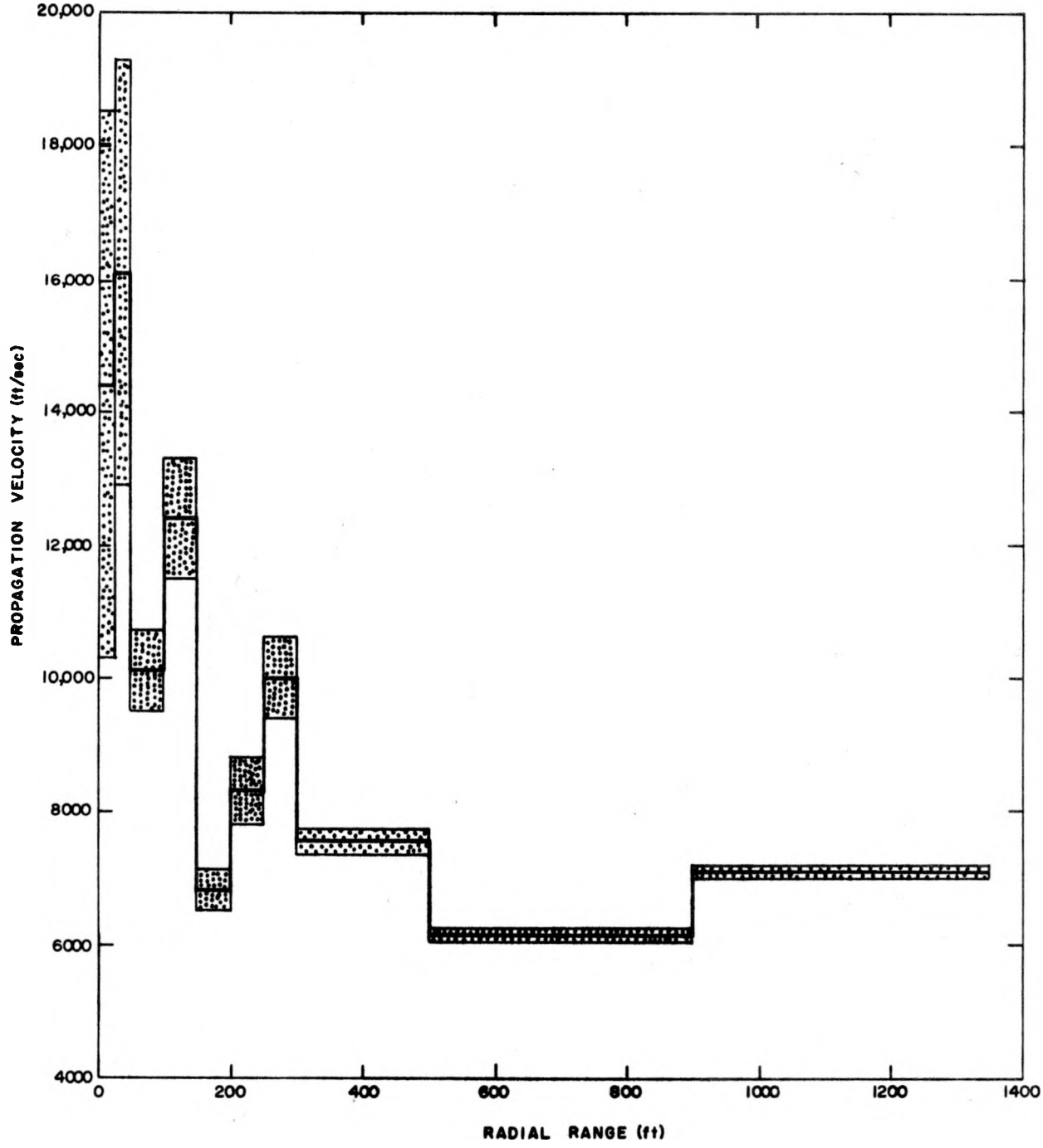

Fig. 6.3—**Propagation velocity-range graph,** horizontal radius.

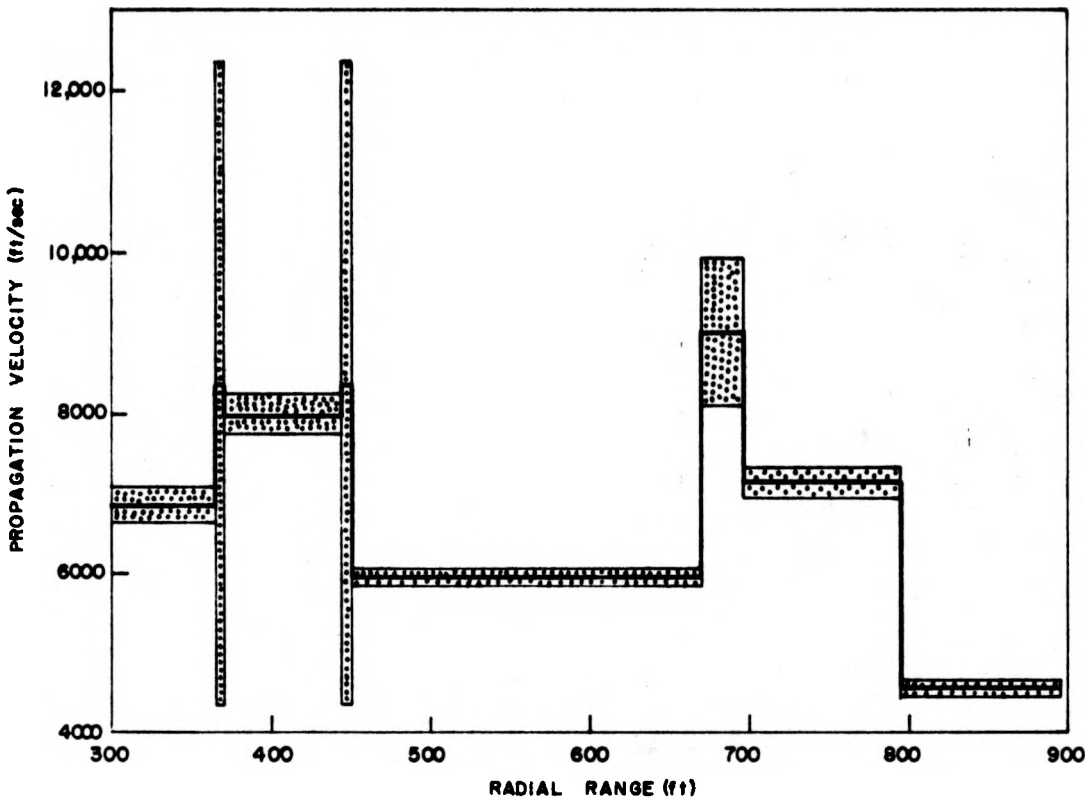

Fig. 6.4—Propagation velocity-range graph, vertical radius.

transition from weak bedded tuff to the welded tuff cap rock and the decrease in velocities in the two 100-foot intervals between the 9,000-ft/sec zone and the surface. This suggests the possibility of continuously decreasing velocity upward from about 9,000 ft/sec near 700 feet to about 3,000 ft/sec near the surface. The importance of this feature of the seismic velocity versus range data will be discussed in the following section.

6.2 ANALYSIS OF MOTION FROM ACCELERATION DATA

Acceleration-time data may be analyzed in several ways to provide insight into motion of the rock after detonation. Peak radial accelerations may be examined as a function of radial range. Acceleration-time data may also be integrated to provide velocity-time and displacement-time data which may also be analyzed as a function of range. Finally, occurrence of specific events other than peak values may be analyzed in terms of radial range and propagation velocities. The first procedure was applied to data from gages on both horizontal and vertical radii; the others were applied to data from all vertical-radius gages and to one gage (AHP-7) on the horizontal radius at the same range as AVS-6, the surface gage of the vertical group.

Peak data from Table 5.1 are plotted versus radial range in Fig. 6.5. Comparison of set ranges with observed peak accelerations (Table 5.1) suggests a rough measure of reliability in terms of saturation degradation of peak values. The outward peak for the gage at 500 feet radial range (AHP-6) was clipped at set range in playback and should have a value perhaps in the 3-to-5-g range. Mechanical deterioration of the magnetic tape on which this channel was recorded precludes obtaining new legible playback records.

Data plotted in Fig. 6.5 indicate that peak accelerations drop off along the horizontal radius approximately as the inverse fourth power of range down to the vicinity of 10 g's, or about 400 feet. The equation statistically derived for this plot,

$$A = 1.78 \times 10^{11} R^{-4}, \qquad (6.1)$$

is rather optimistically presented; overranging of the gages does not justify three significant figures in the coefficient. However, a fair estimate based on the instrumentation and data is that the power of R, -4, is good within 20 percent, and the coefficient 1.78×10^{11} may be low by a power of 10 or more.

These data indicate that the curve departs from linearity for accelerations less than about 10 g, the exponent of range approaching minus two. However, data from overranged gages at 900 and 1,335 feet from zero and the clipped peak at 500 feet range imply that these data points are all too low and that the nonlinearity (shown dashed in Fig. 6.5) should begin at greater accelerations; at 1,355 feet range the peak acceleration, 0.6 g, should be increased to about 2.6 g in agreement with that from USC&GS Station 05 at about 1,340 feet range.

Explosive release of energy within a very small volume in an extensive solid medium, as represented by the Rainier event, may be treated theoretically as a point source problem. Porzel et al[14] have shown that, for such a source, in material having the characteristics of Oak Spring tuff, peak overpressures in the shock wave from a 1-kiloton nuclear explosion will vary with the inverse seventh power of radius for a very short distance from the detonation point. At a relatively small radial range, this attenuation decreases to the inverse third power and, at some larger distance, decreases continuously toward the inverse first power.

Conservation of momentum requires that, for overpressure p in a medium of density ρ, the relation

$$\partial p/\partial r = \rho \partial u/\partial t$$

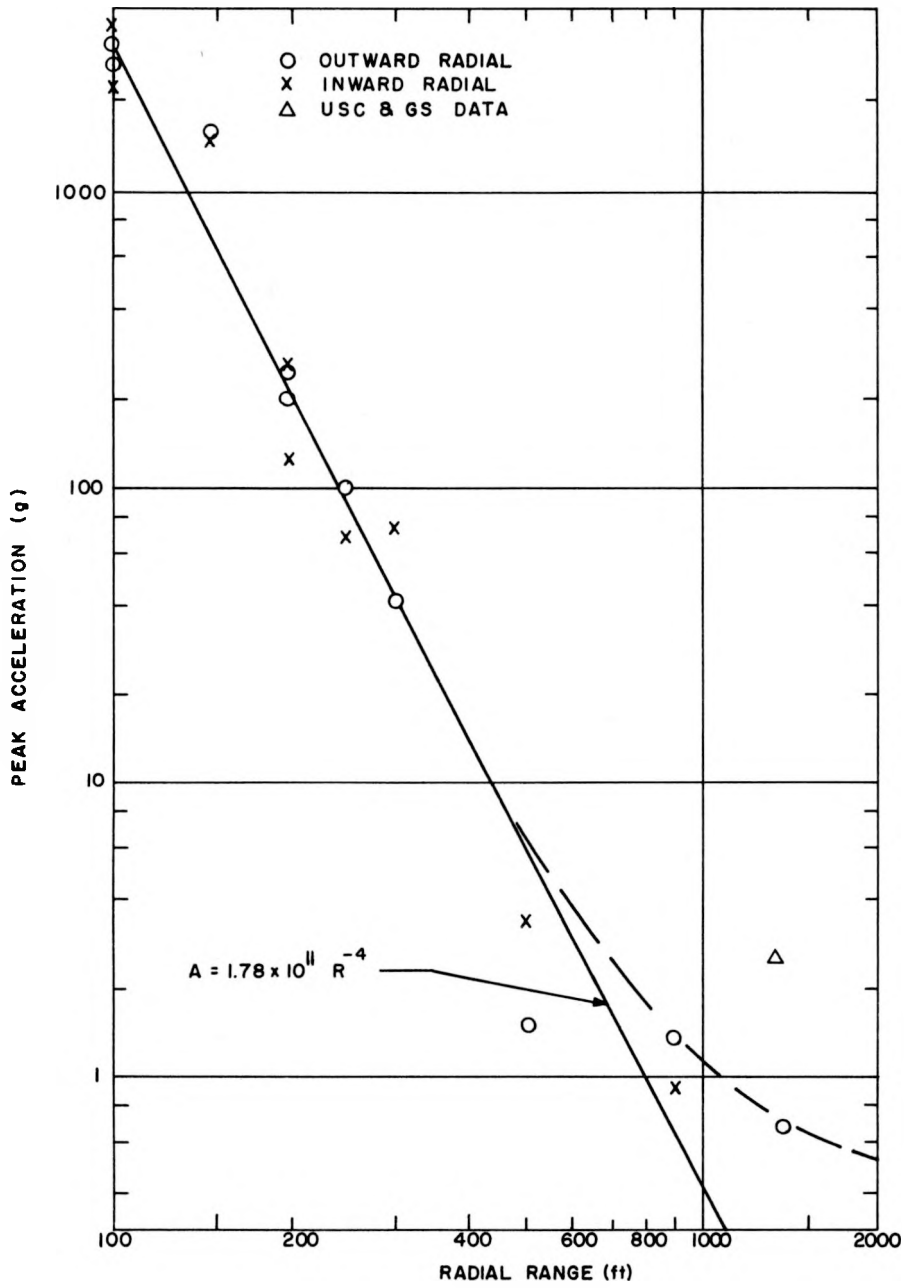

Fig. 6.5—Acceleration-range graph, horizontal radius.

must exist between pressure and particle velocity, u, where r is radial range and t is time. It follows from this equation that acceleration, $\partial u/\partial t$, is proportional to $\partial p/\partial r$.

Thus, point source theory as developed for a completely contained nuclear explosion implies that acceleration must decrease with the inverse fourth power of radial range from about 75 feet (for Rainier event) to about 350 feet, where the rate of attenuation will begin to decrease gradually toward the inverse square of range. This is exactly the sort of attenuation indicated by the data from Project 26.4b accelerometers on the horizontal radius from Shot Rainier (Fig. 6.5).

Data from gages on the vertical radius are not so easily understood. Peak accelerations plotted versus range on logarithmic scales (Fig. 6.6) indicate degradation of peak accelerations with increasing range to about 700 feet, followed by enhancement of acceleration peaks with range up to the surface at about 900 feet range. Corrected peaks (see Section 5.5) for the shallower gages (squares) and SRI peaks (triangles) were used to define the enhancement curve. Transition from decreasing to increasing peak accelerations as a function of range occurs in the vicinity of the transition from loosely cemented tuff to the welded rhyolitic tuff of the cap rock.

The analytical expression for the acceleration-distance curve to 700 feet,

$$A = 1.83 \times 10^{6} R^{-2}, \qquad (6.2)$$

differs markedly from Equation 6.1 for horizontal-radius gages. There is no obvious reason for this difference, but weakness of the rock throughout the lower portion of the vertical radius to about 400 feet from zero may have absorbed energy at a more rapid rate than did the stronger rock along the horizontal radius. In fact, if peak accelerations at 100-foot range are assumed to be similar on the vertical radius to those observed at the same horizontal radius, data from AVS-1X indicate that peak accelerations closer than 370 feet on the vertical radius fall off as the -4.5 power of radius versus -4 for the same region of the horizontal radius. Then that portion of the curve (Fig. 6.6) between AVS-1 (366 feet) and AVS-3 (650 feet) may correspond to the flatter portion of the Fig. 6.5 curve near 900 feet.

Analysis of motion along the upper portion of the vertical radius is based on consideration of parameter-time curves and relative times of various events indicated on these curves (Fig. 5.8). The principal events common to all records from vertical-radius gages within 250 feet of the surface are: (1) a sharp upward acceleration pulse, (2) a prolonged period of downward acceleration nearly constant at about -1 g (free-fall), and (3) a rebound pulse of upward acceleration followed by damped oscillations. Time relationships between these events are given in Table 5.2 and are plotted as functions of range in Figs. 6.2 and 6.7. Certain relations of importance to analysis are evident.

Rise times, as defined by differences between first arrivals and peak times, increase with increasing radial range, in accordance with the dispersive nature of the medium. Rise time for AVS-4 does not follow the established pattern, but poor definition of the first peak (amplifier saturation) gave this record poorer than average precision for this interval.

Secondary upward acceleration peaks are evident in nearly all records for the vertical radius. Records in which definition is good include several of these secondary peaks before the first negative acceleration maximum. Time differences between first peaks and the principal secondary peaks differ slightly between records (41 to 51 milliseconds). However, presence of such a peak in the record from AVS-6 at the ground surface and nearly constant difference between peaks for all gages in the uppermost 225 feet denies interpretation of the secondary peaks

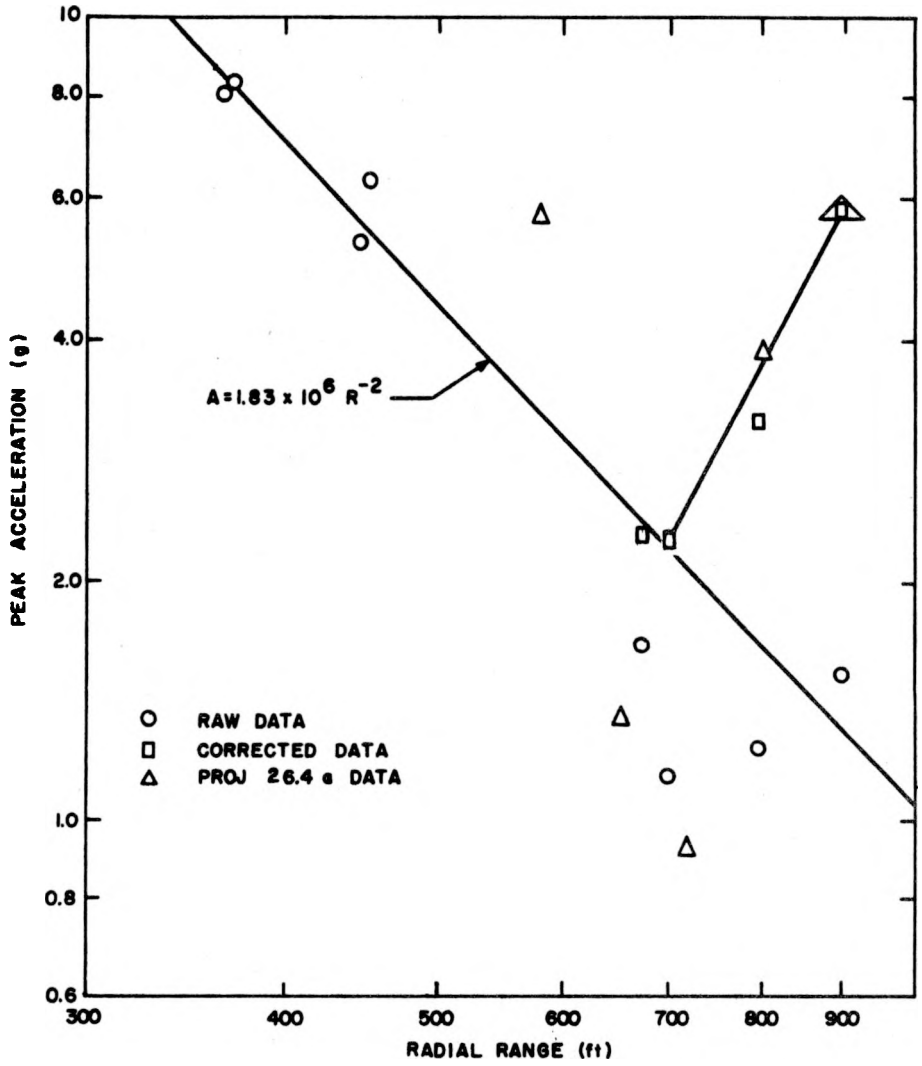

Fig. 6.6—Acceleration-range graph, vertical radius.

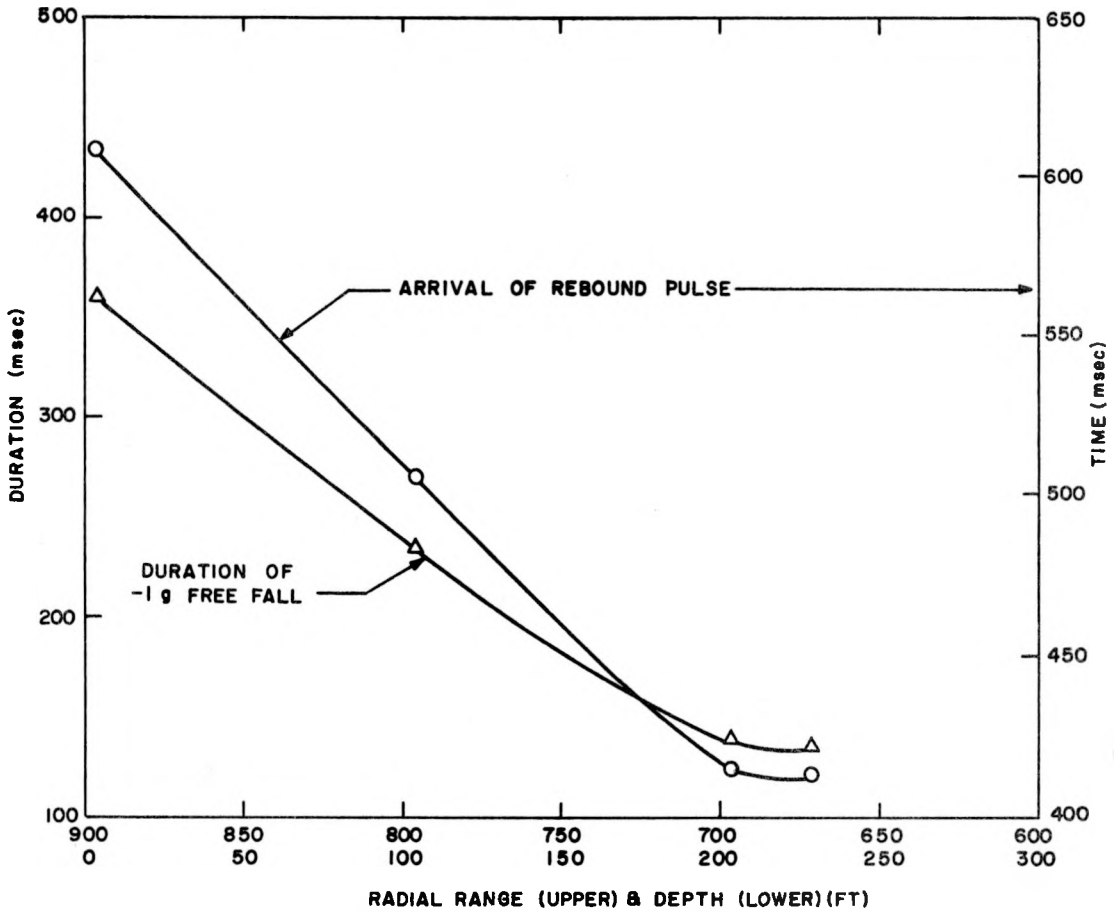

Fig. 6.7—Free-fall duration and rebound arrival versus range.

as reflections from the free surface. These second peaks probably represent an event which occurred shortly after detonation in the vicinity of zero or below it. This could have been collapse of the tunnel or strong reflections from a deeper rock stratum.

Evidence of reflected energy from the free surface is present, however, in most acceleration curves (Fig. 5.8) as distinct changes (upward) in slope at times very nearly coincident with computed arrival times for a surface-reflected pulse. The predicted arrivals are indicated on the curves of Fig. 5.8. The corresponding signals are not all sufficiently strong to appear distinctly in the figure. Three of the deeper gages (AVS-1, AVS-2, and AVS-2X) do not show reflection arrivals, probably because the signal is too weak for recognition at those gages or because it was absorbed at a horizontal parting above them. The effect of these reflected pulses is minor in all gages except AVS-5, the shallowest for which a delayed reflection signal might be expected. The record for this gage shows a distinct secondary upward peak starting at 162 milliseconds and rising at least 0.2 g, and possibly as much as 1 g, above a projected first-pulse decay curve. Reflection must also have affected the peak acceleration at AVS-6 (within 1 foot of the surface), but this probably caused doubling (more or less) of the incident peak to give the corrected 5.8-g peak value.

The period of nearly constant negative (downward) acceleration represents free fall during which the net acceleration is zero (acceleration of -1 g represents cancellation of the acceleration of gravity which constitutes a positive bias on the recording system as calibrated). There is no evidence of free fall in records from ranges less than 671 feet. In fact, negative accelerations in records for deeper gages (AVS-1 to AVS-2X) are considerably greater than 1 g. Free fall begins at times progressively later at deeper gages (ninth column of Table 5.2), but at intervals shorter than those between first arrivals. In fact, all time differences are within the range of error in reading onset of the -1 g portion of curves. Thus, free fall may occur simultaneously for all shallow gages, although this is not definitely established.

Free-fall periods end with rebound pulses (column 10 of Table 5.2), which occur earlier at progressively deeper gages (Fig. 6.7). The rebound pulses at different gages appear to represent different events except in the case of gages AVS-3 and AVS-4. The time interval between initiation of rebound pulses for that pair of gages agrees, within observation errors, with that for first arrivals and implies a pulse traveling upward at seismic velocity, about 9,000 ft/sec. However, data for the two shallower intervals, AVS-4 to AVS-5 and AVS-5 to AVS-6, imply velocities about one sixth of the first-arrival seismic velocities. These facts suggest that rebound data derive from three separate events: (1) termination of free-fall somewhere below AVS-3, as a layer of rock including AVS-3 and AVS-4 comes in contact with rock beneath the parting; (2) a similar event involving a layer parted between AVS-4 and AVS-5 and containing the latter gage; and (3) a third layer parted between AVS-5 and AVS-6 and extending to the surface.

Duration of free fall increases with range (Fig. 6.7). The free-fall phase actually represents both upward and downward motion; the former, a period of decreasing upward velocity, the latter, one of increasing downward velocity. Transition from upward to downward motion is marked by crossover of the particle velocity curve (integrated acceleration) from positive to negative values and marks the time of maximum upward displacement.

Acceleration-time data from vertical radius gages were integrated, as previously suggested, to give velocity-time and displacement-time information. Use of raw data for this operation resulted in obviously invalid results because of the saturation of peak accelerations. Corrected data, derived as described in Section 5.5, were also integrated with more reasonable results. Figure 6.8 shows the results of the first integrations (velocity versus time) for gages on the vertical radius. Solid lines represent velocities derived from raw data, and dashed lines represent those derived from corrected accelerations. Similarly, Fig. 6.9 presents results of the second integration, or displacements versus time. In a few cases, curves obtained from raw data are discontinued after it becomes evident that they are incredible.

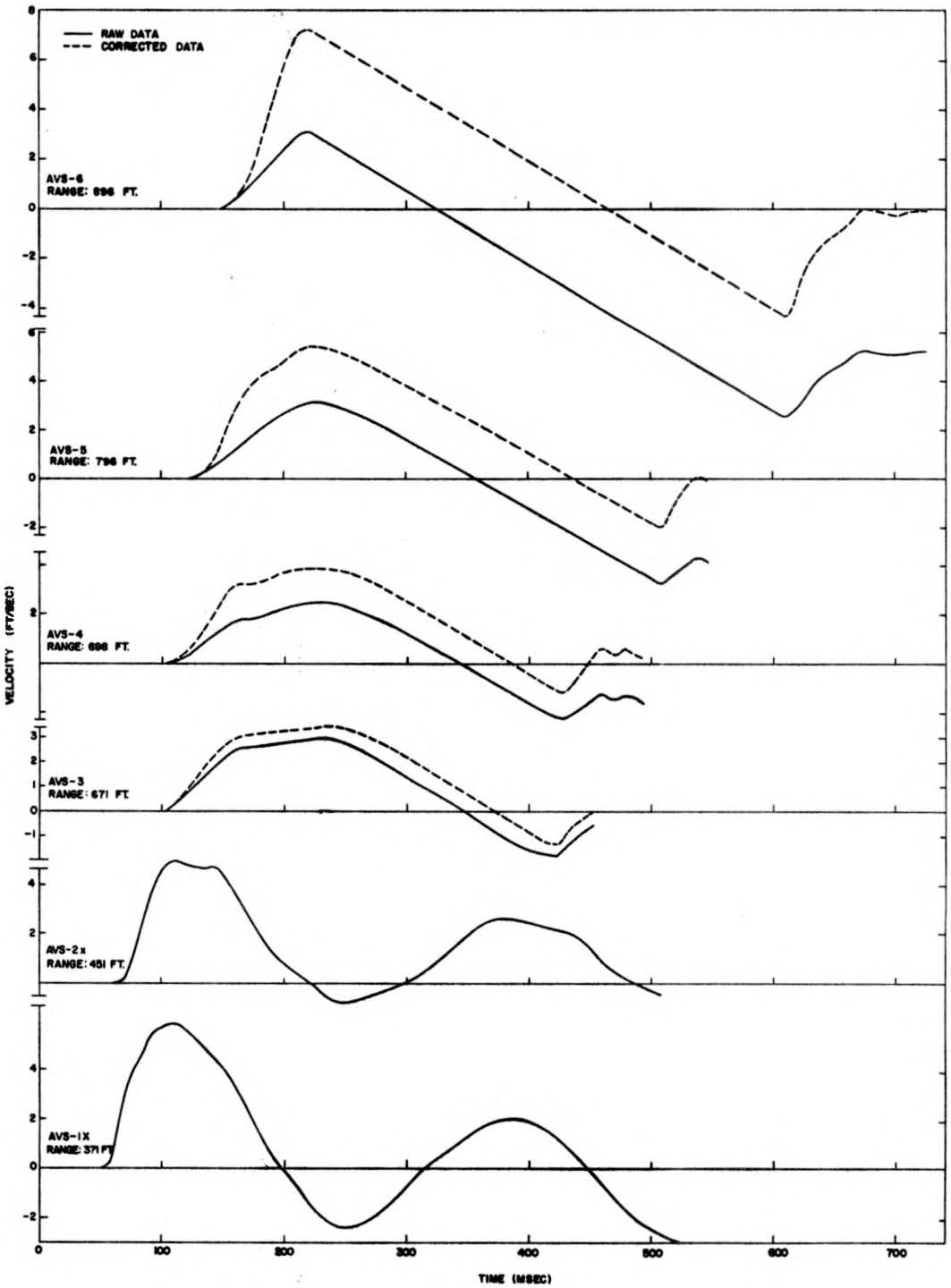

Fig. 6.8—Particle velocity-time curves, vertical radius.

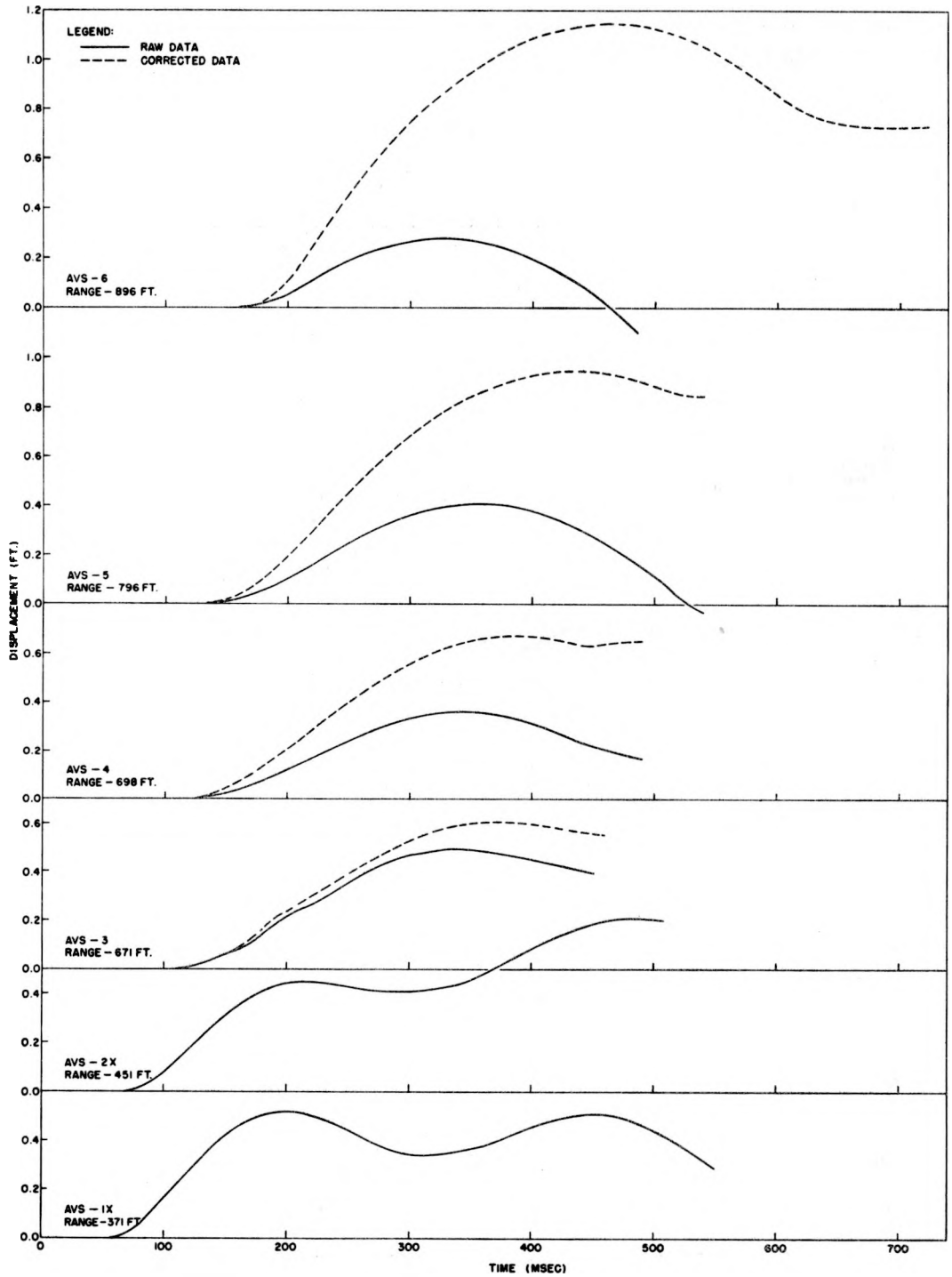

Fig. 6.9—Displacement-time curves, vertical radius.

Pertinent data from the velocity and displacement curves are listed in Tables 6.2 and 6.3. Uncorrected downward peak velocities (Table 6.2) for the shallower gages, in particular AVS-5 and AVS-6, indicate the adverse effect of the clipped peaks. The downward velocity of 8.45 ft/sec for AVS-6 required a downward displacement greater than 1.6 feet as compared with the upward peak displacement of only 0.28 foot. Corrected values (parenthetic in the tables) are reasonable and probably within 20 percent of the real peak values.

A logarithmic plot of peak velocity versus radial range (Fig. 6.10) is roughly similar to that for peak accelerations (Fig. 6.6). Data from the deeper gages decrease roughly as the inverse first power of range, while those from shallower gages (above the deepest parting) increase. As in the case of acceleration, increasing velocity toward the free surface does not follow from an obvious relationship to the free surface.

A similar plot of peak displacements (Fig. 6.11) is roughly similar to the corresponding plot for accelerations, but with flatter slopes both for the deeper and for the shallower phases of the plots. Again, no real significance is attached to the apparent linear relationship in the logarithmic plot for shallower gage data.

The foregoing discussion gives no reason for anticipation of an increase in peak acceleration between the base of the cap rock and the mesa top. However, one possible mechanism for the enhancement seems worthy of at least cursory examination. Seismic transmission of energy in rock is analogous in many respects to acoustic transmission in fluids. Reflections of compressional waves occur at boundaries between media of different density or rigidity in both cases, and the process is controlled in an analogous manner in each.

A compressional wave impinging normally on the boundary between media generates a reflected wave and a transmitted one. Certain equilibrium conditions must be fulfilled at the boundary; algebraic sums of incident and reflected pressures and displacements in medium 1 must equal transmitted pressures and displacements in medium 2. These boundary conditions define for the transmitted wave of amplitude, A_2, the relationship

$$A_2 = A_1 \, 2\rho_1 c_1/(\rho_1 c_1 + \rho_2 c_2)$$

where A_1 is amplitude of the incident wave
ρ_1 is bulk density of medium 1 in which the incident wave occurs
c_1 is seismic velocity in medium 1
ρ_2, c_2 are the corresponding parameters in medium 2 in which the transmitted wave is propagated.

The product, ρc, is defined as the seismic impedance analogous to acoustic impedance.

Evidently, if $\rho_1 c_1$ is greater than $\rho_2 c_2$, A_2 will be greater than A_1. Thus, reflection at a boundary where transmission is into a medium of lower impedance requires enhancement of the peak displacement. Peak accelerations for the postulated type of motion are, in the first approximation, proportional to peak displacements, the proportionality factor being the square of angular frequency. Since, in the first approximation, frequency will not change on reflection, peak accelerations may be expected to follow the same pattern as peak displacement. It should be noted here that peak power transmission at such a boundary follows a quite different pattern, resulting in attenuation of power from incident to transmitted wave.

Seismic velocities, determined from arrival-time differences between gages along the vertical radius above Rainier, show a consistent decrease from the interval between AVS-3 and AVS-4 at 671 to 698 feet range to the interval between AVS-5 and AVS-6 at 796 to 896 feet range. Data from other projects confirm this pattern and suggest that, through the welded tuff cap rock, the velocity decreases upward in a roughly continuous manner from about 10,000 ft/sec at the base to about 3,000 ft/sec at the ground surface. Data from cores show that, through the cap rock, bulk density is roughly constant. Therefore, propagation of a seismic wave upward through the cap rock implies a propagation path along which the seismic impedance decreases

TABLE 6.2—PROJECT 26.4a - VELOCITIES - VERTICAL RADIUS

Gage	Radial range (ft)	Peak upward velocity (ft/sec)	Up peak time (msec)	Cross-over time (msec)	Peak downward velocity (ft/sec)	Down peak time (msec)
AVS-1	366	5.50	112	198	-	-
AVS-1X	371	5.84	111	199	2.42	251
AVS-2	446	4.40	106	200	-	-
AVS-2X	451	4.96	109	221	0.77	250
AVS-3	671	2.99 (3.46)	233	372	1.83 (1.36)	422
AVS-4	698	2.48 (3.86)	233	385	2.24 (1.14)	428
AVS-5	796	3.14 (5.39)	227		4.23 (1.98)	509
AVS-6	896	3.09 (7.26)	219	466	8.45 (4.28)	610

NOTE: Peak values in parentheses are derived from acceleration data corrected by correlation of the AVS-6 record with that for the corresponding SRI (Project 26.4a) record.

TABLE 6.3—PROJECT 26.4b - DISPLACEMENTS - VERTICAL RADIUS

Gage	Radial range (ft)	Peak upward displacement (ft)	Upward peak time (msec)
AVS-1	366	0.485	199
AVS-1X	371	0.513	199
AVS-2	446	0.360	200
AVS-2X	451	0.446	221
AVS-3	671	0.496 (0.607)	347 (371)
AVS-4	698	0.361 (0.671)	344 (385)
AVS-5	796	0.405 (0.947)	357 (437)
AVS-6	896	0.281 (1.15)	334 (463)

NOTE: Peak values and times in parentheses are derived from acceleration data corrected by correlation of the AVS-6 record with that for the corresponding SRI (Project 26.4a) record.

in a roughly continuous manner. This, in turn, suggests a continuous reflection process with increasing displacement and acceleration amplitudes. A quantitative examination of this model requires a more comprehensive study than seems justified because of the uncertainties in Project 26.4b data inherent in overranged instrumentation.

A comparison was made (Fig. 6.12) between data from AVS-6, situated about 900 feet vertically above the burst point within 0.5 foot of the surface, and AHP-7, situated beneath the tunnel floor 900 feet horizontally from the burst point and 765 feet from the tunnel portal. Raw and corrected data for both gages and for the three parameters (acceleration, velocity, and displacement) are included in the comparison. These graphs point out the very marked difference in characteristics of the motion at the two stations. This difference is probably caused principally by reflection doubling at the free surface and free-fall effects along the vertical radius. Weaker rock along the vertical radius, as compared to that along the tunnel, may also affect the peak acceleration pattern along the two radii. There is obviously no free fall at the AHP-7 station in the tunnel.

Transient displacement during the first 500 milliseconds at AHP-7 is only 0.2 foot, appreciably less than the residual displacement at this station indicated by postshot surveys. However, gross effects such as motion of the rock at AHP-7 must have occurred through a period of at least several seconds rather than a half second. Integration of the AHP-7 record over a period of about 3 times that included for this report is feasible and might improve the comparison.

6.3 ANALYSIS OF STRAINS FROM RELATIVE-DISPLACEMENT DATA

Relative-displacement gages mounted on the tunnel wall survived for only a short interval after zero time, in terms of time required for mass motion of the rock (Table 5.3). Consequently, maximum excursions of the displacement curves (Fig. 5.7) represent only an insignificant portion of the real motion, which must have lasted much longer. Some of the records, particularly that for DP-2, represent such violent motion, at rise times too fast to be considered true gage signals in some cases, that much of the signal must be attributed to either circuit failure caused by crushing of the cables or snapping of unprotected gage wires by spalling rock. Estimates of maximum observed strain, ignoring the more radical record peaks, are included in Table 5.3. No meaningful trend can be derived from these data, which represent only the start of motion.

Data from relative-displacement gages on the vertical radius are more complete than those from the tunnel (Fig. 5.9). Only one record, DS-2, is incomplete; a result of FM oscillator malfunction which occurred when ground shock reached the recording trailer. The gage, DS-1, which spanned radial ranges 371 to 381 feet, showed an initial compressive strain of 0.14 percent followed by a nearly equal tensile strain and a residual compressive strain of about half peak value.

Initial compressive strains indicated by gage DS-2, spanning ranges 673 to 683 feet, and DS-3, spanning 676 to 696 feet, are identical 0.06 percent. However, tensile strains for the two gages are very different; the shorter span showing only 0.02 percent, the longer span 0.11 percent. This result suggests that rock within the longer span included a parting or a portion of a zone within which parting occurred.

Tensile strains indicated by the vertical radius gages were subject to a serious limitation because the supporting cables (1/4-inch-steel aircraft-type) were much stronger in tension than either the rock or grout and would probably have restrained the gage at the expense of shearing the surrounding grout. These strains are, therefore, considered to be low.

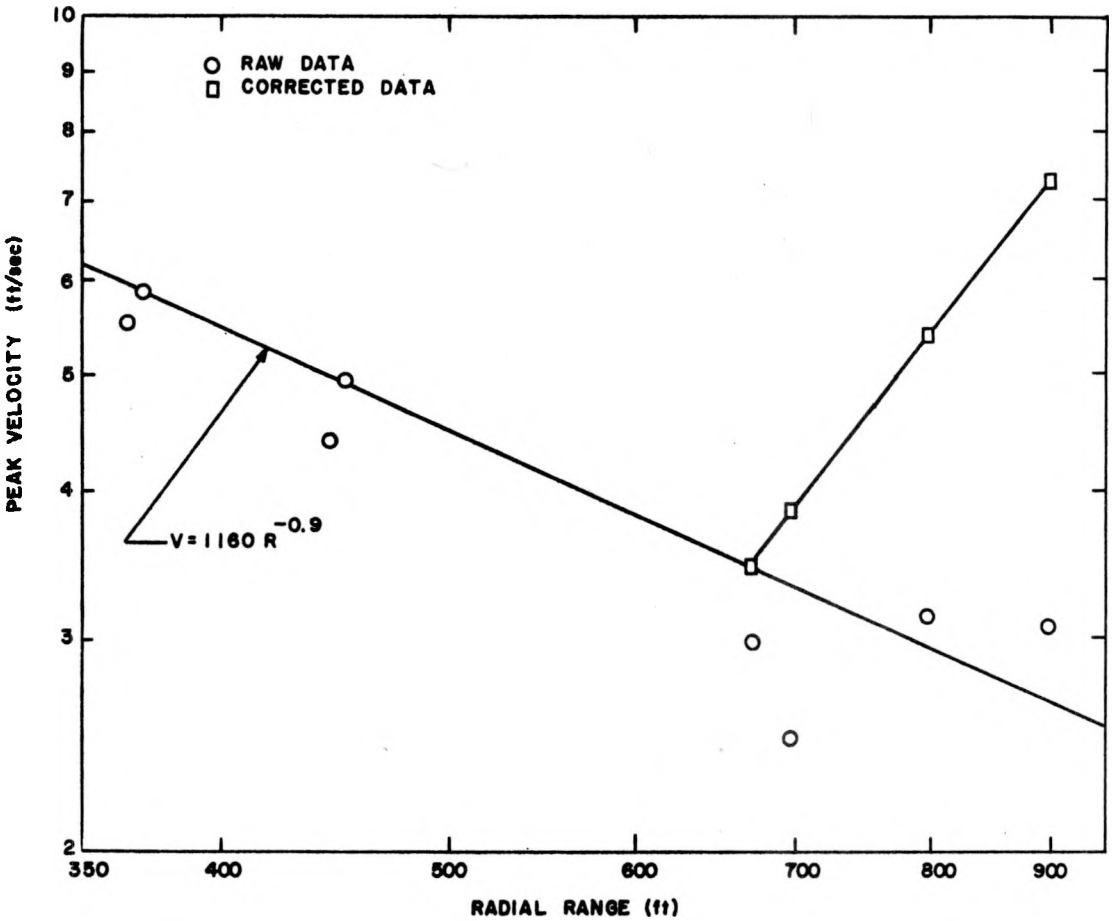

Fig. 6.10—Particle velocity-range graph, vertical radius.

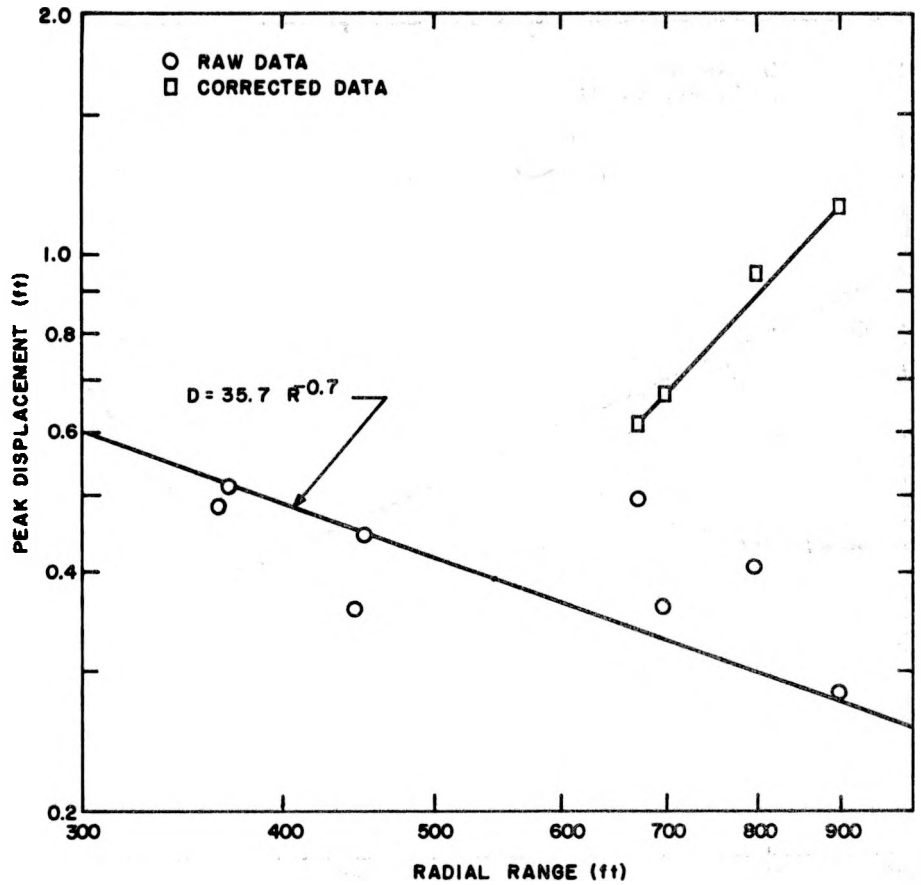

Fig. 6.11—Displacement-range graph, vertical radius.

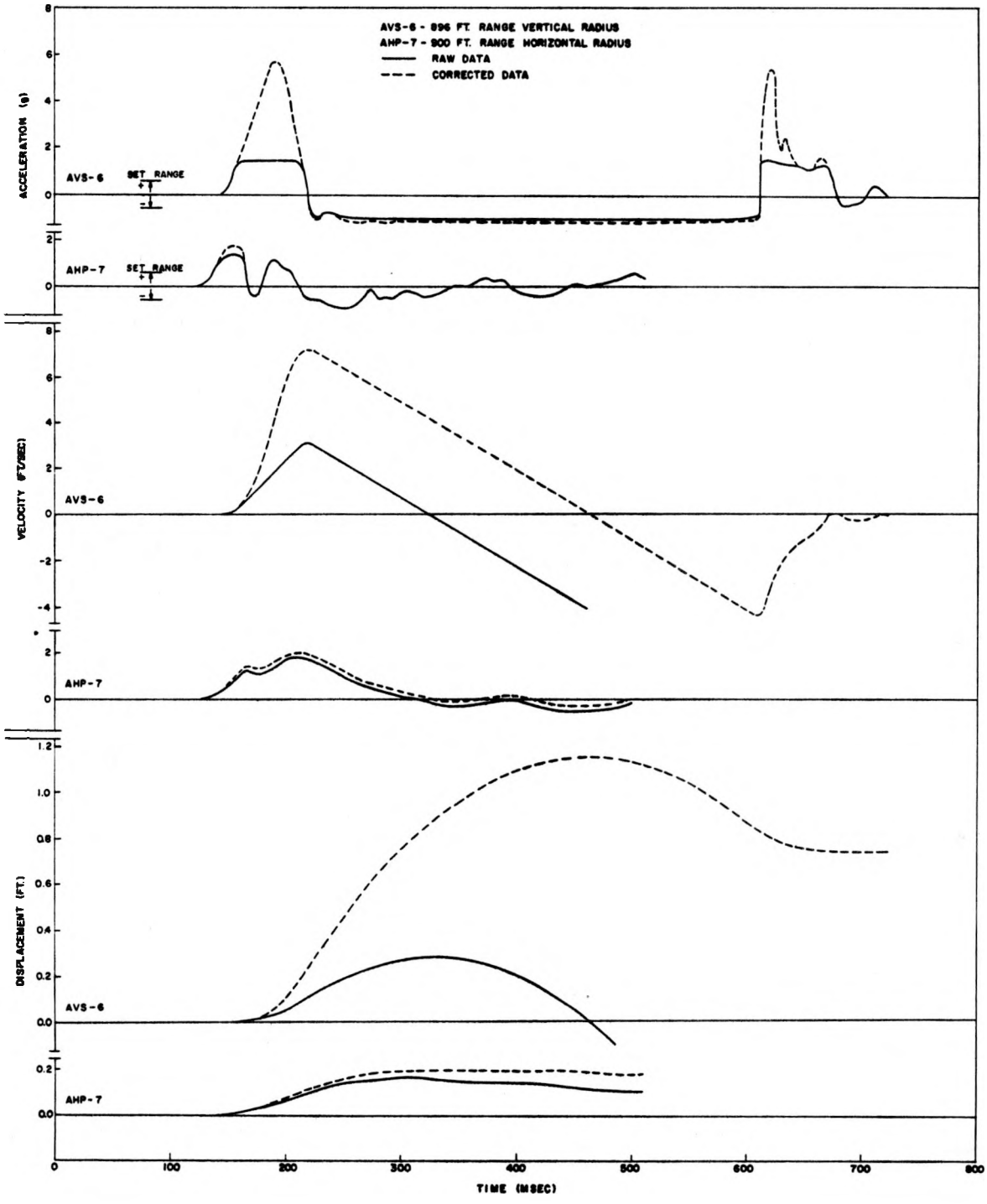

Fig. 6.12—Comparison of motion data at 900 feet range on horizontal and vertical radius.

Chapter 7

CONCLUSIONS AND RECOMMENDATIONS

7.1 CONCLUSIONS

Project 26.4b obtained data concerning strong motion in the rock surrounding Rainier shot at distances ranging from 100 feet to the mesa surface. Much of the information obtained was limited in usefulness by overranged gages, but a number of pertinent trends and some useful information have resulted from analysis of the data.

1. Propagation velocities on the horizontal radius roughly parallel to U-12-b tunnel range from 16,000 ft/sec near 25 feet from burst point to about 7,100 ft/sec near the tunnel portal. Velocities are averages derived for the intervals between gages and show some irregularities reflecting local changes in rock properties. Propagation velocities on the vertical radius range from about 9,000 ft/sec near the transition from massive bedded tuff to the welded tuff cap rock to less than 4,500 ft/sec near the surface. The latter represent seismic velocities, but the very high close-in values indicate shock rather than seismic propagation.
2. Peak accelerations on the horizontal radius fall off approximately as the inverse fourth power of the radius to the vicinity of the 10-g range. Beyond this, the rate of peak degradation drops continuously toward the inverse square of radial range.
3. Peak accelerations and derived velocity and displacement peaks were attenuated up to the base of rhyolitic cap rock where the pattern was reversed. Attenuation was at a lower rate than on the horizontal radius, possibly because of greater energy dissipation in weaker rock along the vertical gage line. Increased acceleration through the cap rock is not directly related to the free surface, but may be related to decreasing seismic impedance upward along the radius from the base of cap rock.
4. Periods of free fall in the acceleration record for gages of the vertical array within the rhyolitic cap rock indicate multiple parting zones, probably at least three, near the base and through most of the cap-rock column. These partings represent a form of spalling.

7.2 RECOMMENDATIONS

One very pertinent recommendation follows from the results of Project 26.4b: A similar study of ground motion on a vertical radius above a deep nuclear explosion should be undertaken in conjunction with surface motion studies, using adequately ranged instrumentation.

It is further recommended, in addition to accelerations, that velocities be observed if suitable gages can be devised and that radial stress and strains be measured at a number of points from the zone of crushing outward to the vicinity of 10-g peak radial acceleration. This would furnish data from which energy absorption as a function of range may be derived.

REFERENCES

1. Keller, G. V., Some Physical Properties of the Oak Spring Tuff (unpublished report), U.S. Geol. Survey, Denver, Colorado, 1957.

2. Perret, W. R. and Preston, R. G., Strong Motion Measurements from a Confined Underground Nuclear Detonation, Operation Plumbbob, ITR-1499, to be published.

3. Sharpe, J. A., The Production of Elastic Waves by Explosion Pressures, Parts I and II, Geophysics 2, pp. 144-154, 311-321, (1942).

4. Underground Explosion Test Program, Final Report, Vol. II, Rock, Engineering Research Associates, April 30, 1953.

5. Griggs, D. T., Notes on Surface and Underground Bursts, Operation Jangle, WT-378 (bound in WT-369), AFSWP, Washington, D.C., April 1952.

6. Morris, W. E. et al, Ground Acceleration Measurements, Operation Jangle, WT-388 (bound in WT-366), Naval Ordnance Laboratory, Silver Spring, Md., June 1952.

7. Swift, L. M. and Sachs, D. C., Underground Explosion Effects, Proj. 1.7, Operation Teapot, WT-1106, SRI, 1957.

8. Sachs, D. C. and Swift, L. M., Small Explosion Tests, Project Mole, Stanford Research Institute, AFSWP-291, Vol. I, December 1955.

9. Diment, W. H. and Dobrovolny, E., Feasibility of Proposed Underground Test, U.S. Geol. Survey, 1957.

10. Warner, S. E., Report on Surface Acceleration Measurements, USGS Shot, NTS, UCRL-4913, Univ. of Calif. Radiation Laboratory, Livermore, Calif., May 15, 1957.

11. Northrop, P. A., Instrumentation for Structures Program, Part I, Scientific Director's Report, Operation Greenhouse, WT-1, January 1951.

12. Perret, W. R., Ground Motion Studies at High Incident Overpressure, Operation Plumbbob, ITR-1405, October 11, 1957.

13. Perret, W. R. and Gentry, V. L., Free-Field Measurements of Earth Stress, Strain, and Ground Motion, Operation Upshot-Knothole, WT-716, February 1955.

14. Porzel, F. B. et al, Study of Blast Effects in Soil, Interim Report No. 5, Armour Research Foundation, Chicago, Ill., May 1, 1958.

PRELIMINARY DISTRIBUTION

1 Brig. Gen. Alfred D. Starbird, DMA
2 Chief, AFSWP, Washington, D. C.
3 Helen Redman, LASL
4 Clovis Craig, UCRL
5 R. G. Preston, UCRL
6 Gene Pelsor, UCRL
7 L. M. Swift, SRI
8 R. V. Whitman, MIT
9 J. D. Shreve, 5112
10 W. R. Perret, 5112
11 W. E. Taylor, 5131

DISTRIBUTION

Military Distribution Category 14

ARMY ACTIVITIES

1 Deputy Chief of Staff for Military Operations, D/A, Washington 25, D.C. ATTN: Dir. of SW&R
1 Chief of Research and Development, D/A, Washington 25, D.C. ATTN: Atomic Div.
1 Assistant Chief of Staff, Intelligence, D/A, Washington 25, D.C.
1 Chief of Engineers, D/A, Washington 25, D.C. ATTN: ENGNB
1 Chief of Engineers, D/A, Washington 25, D.C. ATTN: ENGEB
1 Chief of Engineers, D/A, Washington 25, D.C. ATTN: ENGTB
2 Office, Chief of Ordnance, D/A, Washington 25, D.C. ATTN: ORDTN
1 Commander-in-Chief, U.S. Army Europe, APO 403, New York, N.Y. ATTN: Opot. Div., Weapons Br.
2 Commanding General, U.S. Continental Army Command, Ft. Monroe, Va.
1 Director of Special Weapons Development Office, Headquarters CONARC, ATTN: Capt. Chester I. Peterson
1 President, U.S. Army Artillery Board, U.S. Continental Army Command, Ft. Sill, Okla.
1 President, U.S. Army Infantry Board, U.S. Continental Army Command, Ft. Benning, Ga.
1 President, U.S. Army Air Defense Board, U.S. Continental Army Command, Ft. Bliss, Tex.
2 Commandant, U.S. Army Command & General Staff College, Ft. Leavenworth, Kansas. ATTN: ALLIS (AS)
1 Commandant, U.S. Army Air Defense School, Ft. Bliss, Tex. ATTN: Dept. of Tactics and Combined Arms
1 Commandant, U.S. Army Armored School, Ft. Knox, Ky.
1 Commandant, U.S. Army Artillery and Missile School, Ft. Sill, Okla. ATTN: Combat Development Department
1 Commandant, U.S. Army Aviation School, Ft. Rucker, Ala.
1 Commandant, U.S. Army Infantry School, Ft. Benning, Ga. ATTN: C.D.S.
1 Commandant, U.S. Army Ordnance School, Aberdeen Proving Ground, Md.
1 Commandant, U.S. Army Ordnance and Guided Missile School, Redstone Arsenal, Ala.
1 Commandant, Chemical Corps School, Chemical Corps Training Comd., Ft. McClellan, Ala.
1 Commanding General, The Engineer Center, Ft. Belvoir, Va. ATTN: Asst. Cmdt, Engr. School
1 Director, Armed Forces Institute of Pathology, Walter Reed Army Med. Center, 625 16th St., NW, Washington 25, D.C.
1 Commanding Officer, Army Medical Research Lab., Ft. Knox, Ky.
1 Commandant, Walter Reed Army Inst. of Res., Walter Reed Army Medical Center, Washington 25, D.C.
2 Commanding General, Qm R&D Comd., QM R&D Cntr., Natick, Mass. ATTN: CBR Liaison Officer
2 Commanding Officer, Chemical Warfare Lab., Army Chemical Center, Md. ATTN: Tech. Library
1 Commanding General, Engineer Research and Dev. Lab., Ft. Belvoir, Va. ATTN: Chief, Tech. Support Branch
1 Director, Waterways Experiment Station, P.O. Box 631, Vicksburg, Miss. ATTN: Library
1 Commanding Officer, Picatinny Arsenal, Dover, N.J. ATTN: ORDBB-TK
1 Commanding Officer, Diamond Ord. Fuze Labs., Washington 25, D.C. ATTN: Chief, Nuclear Vulnerability Br. (230)
2 Commanding General, Aberdeen Proving Grounds, Md. ATTN: Director, Ballistics Research Laboratory
1 Commanding General, Army Rocket and GM Agency, Redstone Arsenal, Ala. ATTN: ORDDW-GMTE
1 Commanding General, White Sands Proving Ground, Las Cruces, N. Mex. ATTN: ORDBS-OM
1 Commanding General, Army Ballistic Missile Agency, Redstone Arsenal, Ala. ATTN: ORDAB-C
1 Commanding General, USA Combat Surveillance Agency, 1124 N. Highland St., Arlington, Va.
1 Director, Operations Research Office, Johns Hopkins University, 6935 Arlington Rd., Bethesda 14, Md.

NAVY ACTIVITIES

1 Chief of Naval Operations, D/N, Washington 25, D.C. ATTN: OP-03EG
1 Chief of Naval Operations, D/N, Washington 25, D.C. ATTN: OP-36
2 Chief of Naval Research, D/N, Washington 25, D.C. ATTN: Code 811
2 Chief, Bureau of Aeronautics, D/N, Washington 25, D.C.
1 Chief, Bureau of Ordnance, D/N, Washington 25, D.C.
1 Chief, Bureau of Ships, D/N, Washington 25, D.C. ATTN: Code 348
1 Chief, Bureau of Yards and Docks, D/N, Washington 25, D.C. ATTN: D-440
1 Director, U.S. Naval Research Laboratory, Washington 25, D.C. ATTN: Mrs. Katherine H. Cass
2 Commander, U.S. Naval Ordnance Laboratory, White Oak, Silver Spring 19, Md.
1 Commanding Officer and Director, Navy Electronics Laboratory, San Diego 52, Calif.
1 Commanding Officer, U.S. Naval Mine Defense Lab., Panama City, Fla.
2 Commanding Officer, U.S. Naval Radiological Defense Laboratory, San Francisco, Calif. ATTN: Tech. Info. Div.
3 Officer-in-Charge, U.S. Naval Civil Engineering R&E Lab., U.S. Naval Construction Bn. Center, Port Hueneme, Calif. ATTN: Code 753
1 Commanding Officer, U.S. Naval Schools Command, U.S. Naval Station, Treasure Island, San Francisco, Calif.
1 Superintendent, U.S. Naval Postgraduate School, Monterey, Calif.
1 Officer-in-Charge, U.S. Naval School, CEC Officers, U.S. Naval Construction Bn. Center, Port Hueneme, Calif.
1 Commanding Officer, U.S. Fleet Training Center, Naval Base, Norfolk 11, Va. ATTN: Sp. Wpns. School
1 Commanding Officer, Nuclear Weapons Training Center, Pacific, Naval Station, San Diego, Calif.
1 Commanding Officer, U.S. Naval Damage Control Tng. Center, Naval Base, Philadelphia, Pa. ATTN: ABC Defense Course
1 Director, Naval Air Experiment Station, Air Material Center, U.S. Naval Base, Philadelphia, Pa.
1 Commander, Officer U.S. Naval Air Development Center, Johnsville, Pa. ATTN: NAS, Librarian
1 Commanding Officer, U.S. Naval Medical Research Institute, National Naval Medical Center, Bethesda, Md.
1 Commanding Officer and Director, David W. Taylor Model Basin, Washington 7, D.C. ATTN: Library
1 Commanding Officer and Director, U.S. Naval Engineering Experiment Station, Annapolis, Md.
1 Commander, Norfolk Naval Shipyard, Portsmouth, Va. ATTN: Underwater Explosions Research Division
4 Commandant, U.S. Marine Corps, Washington 25, D.C. ATTN: Code A03H

AIR FORCE ACTIVITIES

1 Assistant for Atomic Energy, HQ, USAF, Washington 25, D.C. ATTN: DCS/O
1 Deputy Chief of Staff, Operations HQ. USAF, Washington 25, D.C. ATTN: Operations Analysis
2 Assistant Chief of Staff, Intelligence, HQ. USAF, Washington 25, D.C. ATTN: AFCIN-IB2
1 Assistant Chief of Staff, Intelligence, HQ. USAFE, APO 633, New York, N.Y. ATTN: Directorate of Air Targets
1 Director of Research and Development, DCS/D, HQ. USAF, Washington 25, D.C. ATTN: Guidance & Weapons Branch
1 The Surgeon General, HQ. USAF, Washington 25, D.C. ATTN: Bio.-Def. Pre. Med. Division
1 Commander-in-Chief, Strategic Air Command, Offutt AFB, Neb. ATTN: Inspector General, Sp. Wpns. Branch, Inspector Division

1 Commander, Tactical Air Command, Langley AFB, Va. ATTN: Doc. Security Branch
1 Commander, Air Defense Command, Ent AFB, Colorado ATTN: Atomic Energy Div., ADLAN-A
1 Commander, Hq. Air Research and Development Command, Andrews AFB, Washington 25, D.C. ATTN: RDRWA
1 Commander, Western Development Division (ARDC) P.O. Box 262, Inglewood, Calif. ATTN: WDSIT, Mr. R. G. Weitz
1 Commander-in-Chief, Pacific Air Forces, APO 953, San Francisco, Calif. ATTN: PFCIE-MB, Base Recovery
2 Commander, AF Cambridge Research Center, L. G. Hanscom Field, Bedford, Mass. ATTN: CRQST-2
5 Commander, Air Force Special Weapons Command, Kirtland AFB, Albuquerque, N. Mex. ATTN: Technical Information Office
2 Director, Air University Library, Maxwell AFB, Ala.
1 Commander, Lowry AFB, Denver, Colorado. ATTN: Dept. of Sp. Wpns. Tng.
1 Commandant, School of Aviation Medicine, USAF, Randolph AFB, Tex. ATTN: Research Secretariat
1 Commander, 1009th Sp. Wpns. Squadron, HQ. USAF, Washington 25, D.C.
3 Commander, Ballistic Missile Division, Wright-Patterson AFB, Dayton, Ohio. ATTN: WCOSI
2 Director, USAF Project RAND, VIA: USAF Liaison Office, The RAND Corp., 1700 Main St., Santa Monica, Calif.

OTHER DEPARTMENT OF DEFENSE ACTIVITIES

1 Assistant Secretary of Defense, Research and Engineering, DOD, Washington 25, D.C. ATTN: Tech. Library
1 Chairman, Armed Services Explosives Safety Board, DOD, Building T-7, Gravelly Point, Washington 25, D.C.
1 Director, Weapons Systems Evaluation Group, Room 1E880, The Pentagon, Washington 25, D.C.
1 U.S. Documents Officer, Office of the United States National Military Representative - SHAPE, APO 55, New York, N.Y.
8 Chief, Armed Forces Special Weapons Project, Washington 25, D.C.
1 Commander, Field Command, AFSWP, Sandia Base, Albuquerque, N. Mex.
1 Commander, Field Command, AFSWP, Sandia Base, Albuquerque, N. Mex. ATTN: FCTG
5 Commander, Field Command, AFSWP, Sandia Base, Albuquerque, N. Mex. ATTN: FCWT
1 Commander, JTF-7, Arlington Hall Station, Arlington 12, Va.

ATOMIC ENERGY COMMISSION ACTIVITIES

3 U.S. Atomic Energy Commission, Classified Technical Library, Washington 25, D.C. ATTN: Mrs. J. M. O'Leary (For DMA)
2 Los Alamos Scientific Laboratory, Report Library, P.O. Box 1663, Los Alamos, N. Mex. ATTN: Helen Redman
15 Sandia Corporation, Classified Document Division, Sandia Base, Albuquerque, N. Mex. ATTN: H. J. Smyth, Jr.
110 University of California Radiation Laboratory, P.O. Box 808, Livermore, Calif. ATTN: Clovis G. Craig
1 Weapon Data Section, Technical Information Service Extension, Oak Ridge, Tenn.
35 Technical Information Service Extension, Oak Ridge, Tenn. (Surplus)